LOWERING RATES OF MORAINE CRESTS FROM ACCUMULATION OF COSMOGENIC ^{36}Cl AND ^{10}Be: EASTERN SIERRA NEVADA, CALIFORNIA

by

J. Scott Shomer

A Thesis Submitted to the Faculty of the

DEPARTMENT OF HYDROLOGY AND WATER RESOURCES

In Partial Fulfillment of the Requirements
For the Degree of

MASTER OF SCIENCE
WITH A MAJOR IN HYDROLOGY

In the Graduate College

THE UNIVERSITY OF ARIZONA

1999

STATEMENT BY AUTHOR

This thesis has been submitted in partial fulfillment of requirements for an advanced degree at The University of Arizona and is deposited in the University Library to be made available to borrowers under rules of the Library.

Brief quotations from this thesis are allowable without special permission, provided that accurate acknowledgement of source is made. Requests for permission for extended quotation from or reproduction of this manuscript in whole or in part may be granted by the head of the major department or the Dean of the Graduate College when in his or her judgement the proposed use of the material is in the interests of scholarship. In all other instances, however, permission must be obtained from the author.

SIGNED: 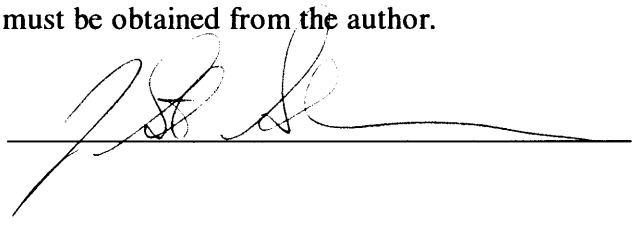

APPROVAL BY THESIS DIRECTOR

This thesis has been approved on the date shown below:

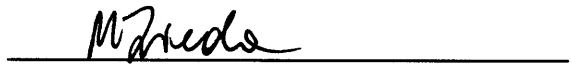

Marek G. Zreda
Assistant Professor of Hydrology and Water Resources

5 Nov. 1999

Date

ACKNOWLEDGEMENTS

I would be negligent if I did not thank the many people who made my thesis and graduate schooling experience what it was. First and foremost, I would like to thank Dr. Marek Zreda for his tireless support. Dr. Zreda's vision of using soil profiles and this particular combination of isotopes for studying landscape evolution was always very clear to him even if I doubted the success of the program. In the end, the success of this study is owed wholly to him.

I could not have added beryllium-10 to the study had Dr. Lal of Scripps Oceanographic Institute not so graciously offered to teach me the extraction process and allowed me the use of his lab for several weeks. His knowledge of the subject is truly inspirational and it was an honor to work, even briefly, with him. A graduate student of Dr. Lal's, Mr. Weiquian Dong, helped me process all my samples in a round the clock, seven days a weeks program and I am much indebted to him as well.

Mrs. Grazyna Zreda helped me to process countless chlorine extractions, make total chlorine measurements, purifications, and was always there to help solve problems in the lab.

Dr. Bull from the Geosciences department was instrumental in getting me into the UofA graduate program and always lent me tremendous support. I am not certain if he knows how much he inspired me, but I hope he reads this by the fire in his new house in New Zealand and can take pride in it. Thank you.

I thank Dr. Long and Dr. Baker for agreeing to be on my committee. They bring a diverse background to the table and will challenge me throughout the remainder of my thesis process.

DEDICATION

This work is dedicated to my friends and family that have supported me through my graduate years. To my mother and father, whose endless support and occasional prodding "when will you be done" has finally taken shape into this document. To my wife, Cynthia, who has always been there to listen to the countless problems encountered and never complained when asked to haul loads of rock and soil samples out of the Sierras.

Lastly, I wish to dedicate this work in loving memory of my Grandfather whose love of the mountains lives on in me.

TABLE OF CONTENTS

LIST OF FIGURES

LIST OF TABLES

ABSTRACT

The accumulation of *in-situ* ^{36}Cl and ^{10}Be in soils from the crests of 11 moraines near Bishop Creek, California was used to determine time-integrated erosion rates and exposure ages. Previous studies have provided the exposure history and estimates of erosion for the Bishop Creek moraine sequence allowing for the validation of the $^{36}Cl/^{10}Be$ model used in this study. With the two isotopes, simultaneous calculations of exposure ages and erosion rates of the soils have been made. Mean erosion rates of the soils calculated using ^{10}Be correlate well with those calculated using ^{36}Cl, and range from 19 to 62 mm/ky. Erosion rates from ^{10}Be have larger uncertainties than those calculated using ^{36}Cl and typically are slightly higher. Meteoric ^{10}Be used in combination with the two *in-situ* isotopes yielded an average ^{10}Be deposition rate (q) of $0.46 \pm 0.16 \times 10^6$ atoms cm^{-2} yr^{-1}, in agreement with previous estimates.

1.0 INTRODUCTION

Knowledge of erosion rates on different temporal and spatial scales is essential in the study of landform evolution. The rates and style of landscape evolution has varied over time in response to climate, sea-level change, uplift, and human disturbance. Knowledge of these rates on multiple time-scales is important in understanding not only how the current landscape was formed, but what will shape the future landscape.

Geomorphologists have used the ammount of sediment leaving a basin to compute an estimate of the lowering rate of the basin and call this rate denudation (Ritter 1967). Denudation is calculated by measuring the physical stream load (Ritter 1967; Summerfield and Hulton 1994), analyzing stream geochemistry to determine chemical erosion rates (Louvat and Allegre 1997), or by utilizing highly detailed terrain models using a GIS system to model present and paleosurfaces (Gunnell 1998; Roessner-Sigrid and Strecker-Manfred 1997), the difference being attributed to denudation.

Denudation rate studies have some shortcomings. A major problem with stream-loading estimates using physical and chemical loading of streams leaving a basin is that they only consider those sediments removed completely from a basin. These models do not allow for sediment to be redistributed within a basin (Ritter 1978) where portions of the basin may actually be agrading. They also must assume that the material removed is derived in equal portions from all areas of the watershed.

Denudation rates computed using detailed digital terrain models are now being calibrated in areas with well known exposure hiostories (Gunnell 1998; Roessner-Sigrid

and Strecker-Manfred 1997). This process requires detailed knowledge of not only current topography but well constrained paleo-topography as well. In areas with complex relief, obtaining accurate values of a paleo-surface's age and location after erosion has removed it can prove difficult (Gunnell 1998).

Short-term erosion rates can be determined by direct measurements. Long-term erosion rates however, are more difficult to determine directly and must be extrapolated from short-term rates. Cosmogenic nuclides can be used to approach the problem of determining erosion rates on different spatial scales and long temporal scales.

The concept of using cosmogenic isotopes in the geological sciences was first proposed over 40 years ago (Davis and Schaefer 1955; Lal et al. 1957). However, potential for utilizing cosmogenic isotopes as a geochronometer could not come to fruition until the late 1980's when the development of accelerator mass spectrometry (AMS) provided the sensitivity necessary to accurately measure the small number of atoms produced by cosmogenic reactions with terrestrial matter (Elmore and Phillips 1987).

Early work focused upon calculating theoretical production rates of cosmogenic isotopes in the atmosphere (Lal et al. 1957) and in the shallow lithosphere (Lal and Peters 1967) Because the incident cosmic-ray flux is modified by the earth's magnetic field and attenuated by the atmosphere changes in latitude and altitude of the surface affect the production rate (Cerling and Craig 1994; Lal and Peters 1967). Scaling factors for the theoretical production rates at a given location relative to the reference location have been developed by Lal (Lal 1991; Lal and Peters 1967).

Cosmogenic isotopes have been measured on independently dated surfaces to determine the production rates and to test scaling factors for the commonly-used cosmogenic isotopes (Lal 1991; Liu et al. 1994; Monaghan et al. 1986; Nishiizumi et al. 1996; Phillips and Elmore 1986; Phillips et al. 1996; Yokoyama et al. 1977; Zreda and Phillips 1994a).

With an understanding of the mechanics of accumulation of isotopes at the earth's surface, cosmogenic isotopes have become a powerful tool for evaluating geologic problems, such as erosion rates (Barg 1992; Lal 1991; Pavich et al. 1985; Zreda and Phillips 1994a), landform dating (Nishiizumi et al. 1991a; Phillips and Elmore 1986; Phillips et al. 1998; Zreda et al. 1999), and paleo-climates (Benson et al. 1996; Dansgaard et al. 1993; Raisbeck et al. 1992).

The practicality of using meteoric ^{10}Be accumulated in soil profiles has been demonstrated (Anderson et al. 1990; Barg 1992; Lal et al. 1996; McHargue and Damon 1991), although there is evidence of mobility and loss of ^{10}Be under certain conditions (Monaghan and Elmore 1994; Monaghan et al. 1983). The feasibility of using accumulation of *in-situ* produced ^{36}Cl for surface exposure dating has been demonstrated using boulders from moraine crests in the Sierra Nevada range (Phillips et al. 1996; Phillips et al. 1990; Zreda, 1994a).

In this study, I develop an approach for determining the exposure age and erosion rates of moraines using *in-situ* ^{36}Cl and ^{10}Be. By utilizing the moraine matrix, I have reduced the number of samples that were necessary in the boulder study (Zreda and Phillips 1994a). I show that in an arid environment accumulation of meteoric ^{10}Be yields

profiles that can be used to determine erosion rates. In addition, I demonstrate the utility of using *in-situ* ^{10}Be and ^{36}Cl with meteoric ^{10}Be in the soil profiles to simultaneously determine exposure ages and erosion rates. Finally, using the two *in-situ* nuclides ^{36}Cl and ^{10}Be and meteoric ^{10}Be also allows an independent assessment of ^{10}Be deposition rates.

2. BACKGROUND

2.1 GENERAL

Cosmogenic nuclides are utilized as tools in many fields of science that require evaluation of time dependent factors. Determining landform ages (Zreda and Phillips 1994b), measuring erosion rates (Lal 1991), and estimating recharge rates (Bentley et al. 1986; Bentley et al. 1982; Davis and Murphy 1987) are just a few applications of cosmogenic isotopes. Because such studies rely upon measuring the accumulation and decay of one or more isotopes, it is critical to know the mechanisms that control their production.

The cosmogenic isotopes ^{36}Cl (half-life of 3.01×10^5 yr) and ^{10}Be (half-life of 1.50×10^6 yr) are produced in the atmosphere (meteoric, atmospheric or "garden-variety") or within minerals (*in-situ*) near the earth's surface when cosmic rays interact with target atoms. Cosmic rays originate from the sun (solar cosmic rays) and from the galaxy (galactic cosmic rays). Solar cosmic rays have low energies, typically from 1 to 50 MeV, with some particles having energies as high as 100 MeV (Cerling and Craig 1994). In contrast, galactic cosmic rays have much higher energies, up to 100 GeV (Cerling and Craig 1994).

Cosmogenic ^{36}Cl and ^{10}Be are produced in the atmosphere and in the upper few meters of the lithosphere. High energy nucleons are created in the uppermost atmosphere by cosmic rays. These high energy nucleons collide with atoms whose atomic structure is broken apart by the incident nucleon. This reaction, known as spallation, splits the

target nucleus into three or more particles. These reactions were first observed by exposing sensitive film at high altitudes. The film is capable of capturing charged particles on the emulsion (FIGURE 2-1).

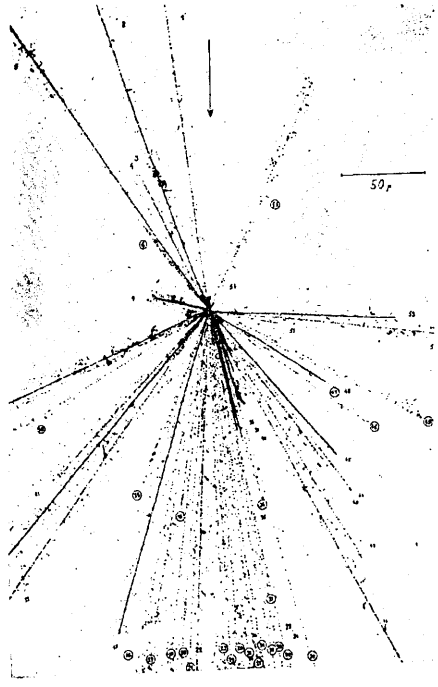

FIGURE 2-1 Spallation reaction captured on electron sensitive film exposed near the top of the atmosphere (Kurz and Brook 1994)

Because the nucleons are slowed by each collision, production of spallogenic nuclides decreases as the nucleons experience multiple collisions. The spallation reaction produces particles with lower energies than the original incident nucleon. These particles create a cascading reaction with other atoms.

There is a marked effect between production rates at the poles, where the atmosphere is thin and the earth's magnetic field is weak, and at the equator where the atmosphere is thicker and the magnetic field strength is much higher (Lal and Peters 1967; Lal et al. 1957). The charged particles are slowed by ionization, but neutrons

travel until they interact with matter or lose energy by inelastic scattering (Lal and Peters 1967). In the shallow subsurface, production of spallogenic nuclides decreases exponentially with depth below the ground surface as nucleons lose energy easily as they move through dense material (Zreda et al. 1991).

2.1.1 Direct measurements of production rates

Both photographic emulsions and thin walled ionization chambers were used in early studies in an attempt to directly measure production rates of cosmogenic nuclides. The first method used very sensitive photographic film exposed during flights near the top of the atmosphere. Charged particles leave a trace of their path on the film. Spallation reactions appear as "stars" in Figure 2-1.

While photographic emulsions were used widely in early studies of nuclear interactions, they cannot be used to directly measure production rates of cosmogenic nuclides in the atmosphere because the film itself has a chemical composition very different from the atmosphere. Lal and Peters (1957) reported that 65 percent of the stars created on the emulsion were due to reactions with silver or bromine nuclei. Production rates in the remaining 35 percent were due to reactions with carbon, nitrogen and oxygen. The values obtained in this type of measurement must be scaled to estimate production rates in the atmosphere at varying locations on the globe.

Despite the limitations of using thin walled ionization detectors to determine star production rates, Lal and Peters used these rates as a basis for calculating the first values for cosmogenic nuclide production rates (Lal and Peters 1967). Lal (1957 & 1968)

considered the effects of atmospheric depth as well as latitude and constructed curves for several of the commonly used isotopes including ^{10}Be and ^{36}Cl (Figure 2-2). Using these calculations and subsequent curves created by Lal (1968), it becomes possible to determine the relative production rates of cosmogenic isotopes on earth. These scaling factors are presented in later sections specific to ^{36}Cl and ^{10}Be.

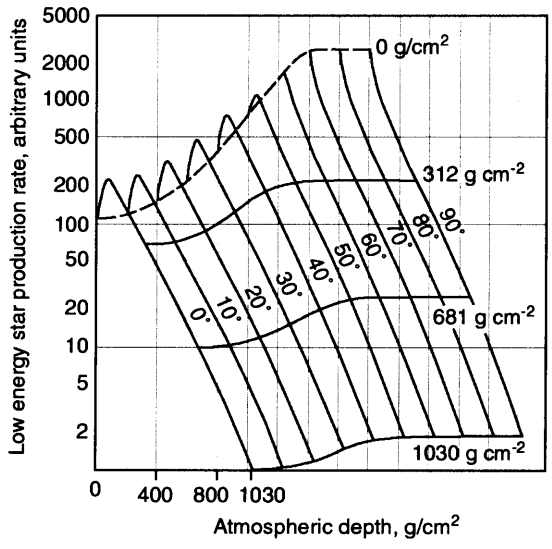

FIGURE 2-2 Star production rates for given atmospheric depths and latitude (Lal and Peters, 1957). Production rates of cosmogenic isotopes are, at first approximation, proportional to the star production rates.

2.2 PRODUCTION MECHANISMS FOR CHLORINE-36

Cosmogenic ^{36}Cl is produced by spallation, by secondary thermal neutron capture and by muon capture (Lal and Peters 1967; Zreda et al. 1991). Spallation involves the splitting of a target nucleus into three or more particles as the result of bombarding nucleons with binding energies of about 8 MeV with energetic particles on the order of 50 MeV or more. In nature, such energies occur only in cosmic rays, and spallation reactions are the primary production mechanisms for nuclides in the atmosphere and surface soil. Spallation reactions are generally negligible below depths of a few meters

because neutrons lose energy quickly on contact with matter (Fabryka-Martin 1988; Zreda and Phillips 1994b).

Slow or thermal neutrons (< 0.025 eV) can be captured by nuclei altering the balance of neutrons and protons in the target element. Most of the isotope producing reactions in the atmosphere can be attributed to thermal neutrons (Lal and Peters 1967). Likewise, neutron capture plays a significant role in *in-situ* production of ^{36}Cl (Zreda et al. 1991; Zreda and Phillips 1994b) and will be discussed in a later section.

Negative muon capture reactions are relatively unimportant at high altitudes, where neutron reactions predominate (Lal 1988), but become increasingly more important at low elevations and in calcic rocks (Lal and Peters 1967; Zreda and Phillips 1994b). Negative muons can penetrate deeper in the lithosphere than neutrons due to their lower reactivity, and become progressively more important below depths 1-2 meters (Fabryka-Martin 1988; Zreda and Phillips 1994b). For the purpose of this study, the effects of negative muon capture in the shallow pits was considered negligible compared to the effects of spallation and thermal neutron reactions.

2.2.1 Production of atmospheric (meteoric) ^{36}Cl

Natural production of ^{36}Cl is due to spallation of ^{40}Ar by high energy protons [$^{40}Ar(p,2n2p)^{36}Cl$] and by absorption of neutrons by ^{36}Ar [$^{36}Ar(n,p)^{36}Cl$] (Bentley et al. 1982; Davis and Murphy 1987). Anthropogenic ^{36}Cl was produced by detonating hydrogen bombs in the shallow atolls of the Pacific Ocean. Meteoric ^{36}Cl is not used in this study, but it is important to know its sources to minimize its presence while measuring the *in-situ* component.

2.2.2 *Production of* in-situ ^{36}Cl

In the top meter of the lithosphere, thermal neutron activation of ^{35}Cl and spallation of ^{39}K and ^{40}Ca are the dominant production mechanisms (Fabryka-Martin 1988; Yokoyama et al. 1977). Below, slow negative muon capture by ^{40}Ca becomes progressively more important (Zreda et al. 1991). Table 2-1 illustrates the relative importance of different reactions allowing for variances due to the chemical composition of the rock.

TABLE 2-1 Production of ^{36}Cl in terrestrial rocks (from Zreda 1991)

Reaction Type	Notation	% of Total ^{36}Cl
Spallation of K	$^{39}K(n,2n2p)^{36}Cl$	16 – 80
Spallation of Ca	$^{40}Ca(n,2n3p)^{36}Cl$	
Thermal neutron activation of Cl	$^{35}Cl(n,\gamma)^{36}Cl$	11 – 80
Negative muon capture by Ca	$^{40}Ca(\mu^-,\alpha)^{36}Cl$	0.3 – 10
Thermal neutron activation of K	$^{39}K(n, \alpha)^{36}Cl$	0 – 2
Negative muon capture by K	$^{39}K(\mu^-,p2n)^{36}Cl$	0 – 0.4

Spallation of potassium [$^{39}K(n,2n2p)\ ^{36}Cl$] and calcium [$^{40}Ca(n,2n3p)\ ^{36}Cl$] is most important in rocks with low concentrations of chlorine (Fabryka-Martin 1988; Zreda et al. 1991). Thermal neutron activation of ^{35}Cl is the dominant production mechanism in rocks with low Ca and K (Fabryka-Martin 1988; Phillips et al. 1996).

Although fast neutrons are attenuated exponentially with depth, some thermal neutrons escape from the lithosphere into the atmosphere and create a decrease in production rate at the lithosphere/atmosphere boundary (Liu et al. 1994; Zreda and

Phillips 1994b). Thus, thermal neutrons have a maximum flux below the lithospheric surface at a depth of approximately 45 g/cm^2 (Liu et al. 1994). Figure 2-3 illustrates the relative production rate of ^{36}Cl for rocks with different chemical compositions (Zreda and Phillips 1994b). The top line is for pure thermal neutron activation of ^{35}Cl and the bottom for pure spallation of ^{39}K and ^{40}Ca. The curves between represent combinations of the two production mechanisms.

Cosmogenic ^{36}Cl surface exposure ages were calculated using CHLOE software (Phillips and Plummer 1996). Spallation production rates of 73.3 ± 4.9 atoms ^{36}Cl per g Ca yr^{-1} and 154 ± 10 atoms ^{36}Cl per g K yr^{-1} (Phillips et al. 1996) were used in the calculation. Thermal neutron activation was calculated (Liu et al. 1994) from the fast neutron production rate of 586 ± 40 neutrons per g air yr^{-1} (Phillips et al. 1996). These values are based on studies of 15 different surfaces at 8 locations, which simultaneously calculated the production rates from Ca, K and Cl at each site (Zreda et al. 1999).

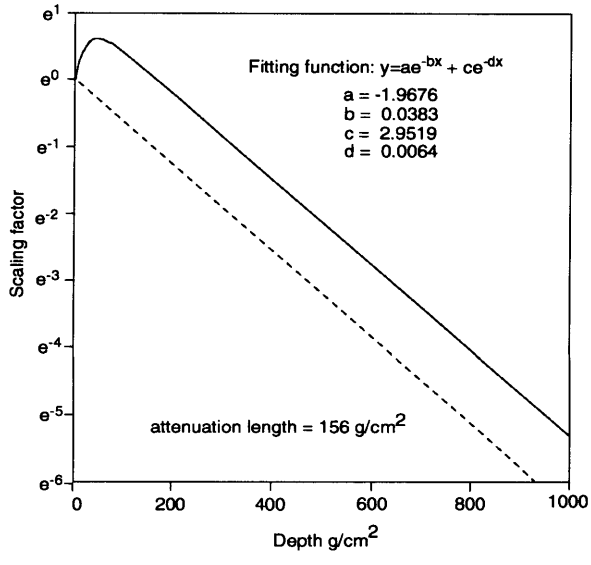

FIGURE 2-3 Depth vs. production from Zreda, 1994. The solid line is for pure thermal neutron activation of ^{35}Cl and the dashed line is for pure spallation of ^{39}K and ^{40}Ca.

2.2.3 Scaling Factors

Elevation, latitude and depth (ELD) affect the production rates of cosmogenic isotopes. The EL correction is a cubic polynomial ($y = a + bx + cx^2 + dx^3$) where x is the elevation above sea level in km and y is the scaling factor (Lal 1991; Zreda and Phillips 1994b). The values for a,b,c and d at various latitudes for ^{36}Cl are shown in Table 2-2. Note that EL =1 for sea level and latitudes above 60°.

TABLE 2-2 Scaling polynomials for cosmogenic production due to neutrons (Zreda and Phillips, 1994b; modified from Lal, 1991)

Latitude	a	b	c	D
0°	0.5790	0.4482	0.1723	0.0359
10°	0.5917	0.4415	0.1944	0.0363
20°	0.6691	0.4764	0.2320	0.0435
30°	0.8217	0.6910	0.1712	0.0822
40°	0.9204	0.8849	0.2487	0.1031
50°	0.9865	1.0298	0.2992	0.1333
60-90°	1.0000	1.0889	0.3105	0.1382

2.3 PRODUCTION MECHANISMS FOR BERYLLIUM-10

2.3.1 Production of Meteoric ^{10}Be

Beryllium-10 is produced at the top of the atmosphere in spallation reactions by cosmic rays incident primarily on nitrogen and oxygen (Pavich et al. 1984). The spallation reaction creates "stars" with 2-3 prongs in nitrogen and 2-4 prong in oxygen (Lal and Peters 1967; Lal et al. 1957).

Production of meteoric ^{10}Be in the atmosphere is not uniform. Lal and Peters (1967) investigated the production rates in the troposphere versus the stratosphere and discovered that most of the cosmogenic nuclides were produced in the stratosphere at high latitudes (Lal and Peters 1967; Lal et al. 1957). In the troposphere, production is only a fraction of what is seen in the upper atmosphere (Fig 2-4). Tropospheric production of ^{10}Be at 30° N is less than half of the production for the entire atmosphere at the same latitude (Lal et al. 1957). The percentage of tropospheric contribution decrease markedly towards the poles.

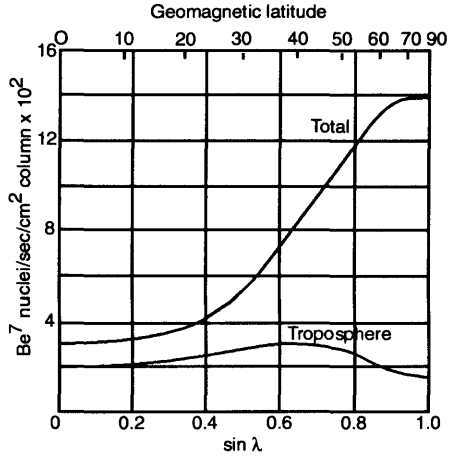

FIGURE 2-4 Tropospheric and total production rate of ^{10}Be (from Lal and Peters, 1957).

Long-lived isotopes, such as ^{10}Be, are not expected to be uniformly distributed in the atmosphere because they are quickly removed as soon as they reach the cloud-bearing strata; their fallout, therefore, depends on latitude (Lal et al. 1957). It should be noted, however, that the tropospheric production rate stays remarkably constant over all latitudes. The effect of higher production rates at higher latitudes is compensated by the decrease in the height of the tropopause (Lal et al. 1957). Averaged over the globe, the production in the troposphere accounts for roughly 30% of the total production. Raisbeck and Yiou (1984), have suggested that there is little contribution of stratospheric aerosols in the tropospheric air indicating a relatively stationary or upward airflow between troposphere and stratosphere (Raisbeck and Yiou 1984). While for isotopes with short half-lives residence time in the atmosphere can play a significant role, it may be considered that compared with the half-life of 1.5 million years for ^{10}Be, its residence time in the atmosphere of months to tens of years is inconsequential.

With the low production rate of ^{10}Be, the ability to measure small quantities of ^{10}Be by accelerator mass spectrometry (AMS) has been even more important for revising production rate estimates of ^{10}Be than for other isotopes. Before the advance of AMS, the global average production was reported as 2.6×10^6 atoms cm^{-2} yr^{-1} (Lal et al. 1957), then revised to 1.42×10^6 atoms cm^{-2} yr^{-1} after correcting for anomalous solar activities affecting the previous data (Lal and Peters 1967). This value has been further refined to 1.3×10^6 atoms cm^{-2} yr^{-1} (Pavich et al. 1986). Monaghan (1983) has reported production rates from California soils as 0.56×10^6 atoms cm^{-2} yr^{-1} and has accounted for the variation in the production rates by explaining that beryllium must me highly mobile and

is therefore lost in the system (Monaghan et al. 1983). It should be noted that Monaghan's study was severely constrained by the lack of good age control for the surfaces studied and by the assumption of zero erosion.

In this study, the ages of the Bishop Creek moraines have already been determined by others (Phillips et al. 1998; Zreda and Phillips 1994a) using *in-situ* accumulation of ^{36}Cl in boulders and will be confirmed using *in-situ* ^{10}Be and ^{36}Cl in soils. The combination of the two isotopes makes it possible to determine both erosion rate and age. Using these ages and erosion rates, an independent calculation of meteoric ^{10}Be deposition rate has been made and will be presented in a later chapter.

2.3.2 Production of in-situ ^{10}Be

Production of ^{10}Be in quartz is much simpler than ^{36}Cl as it is formed primarily by the interaction of high-energy neutrons with ^{16}O [^{16}O (n, 4p3n) ^{10}Be] (Nishiizumi et al. 1989). Smaller contributions relative to the neutron production arise from nuclear interactions with protons (≤10%) and with negative muons (~16%) (Nishiizumi et al. 1989). At depths below 1-2 meters in the lithosphere, the influence of negative muons becomes increasingly more important (Lal 1991; Nishiizumi et al. 1996; Nishiizumi et al. 1989). The shorthand notation for the negative muon reaction is: ^{16}O (μ^-,3p3n) ^{10}Be.

Quartz is an ideal material for ^{10}Be studies because of its simple target chemistry, its abundance in nature and its resistance to weathering (Kurz and Brook 1994). The resistance of quartz to chemical weathering also allows individual grains to be leached in hydrofluoric acid to remove any potential meteoric ^{10}Be (Kohl and Nishiizumi 1992).

The production rates of *in-situ* ^{10}Be, originally computed by Lal (1967), have been determined using glacially polished bedrock in the Sierra Nevada by Nishiizumi *et al.* (1989). The latitudes and altitudes of the calibration are very similar to the Bishop Creek location used in this study. For 44° N and 3.3 km above sea level the ^{10}Be production rate was calculated to be 62±3 atoms g^{-1} yr^{-1} (Nishiizumi et al. 1989) which translates into approximately 6 atoms g^{-1} cm^{-1} at sea level and high latitudes.

Once the production rate (P) is known at the sampled altitude and latitude, the following equation for concentration of ^{10}Be is used to calculate either erosion rate (ε) or exposure age (t) (Nishiizumi et al. 1991a):

$$N = P/(\lambda + \rho\varepsilon/L)\,(1 - e^{-(\lambda + \rho\varepsilon/L)t})$$

where N is the measured ^{10}Be concentration (atoms $(g\ SiO_2)^{-1}$), t is the exposure time (yr), ε is the erosion rate (cm yr^{-1}), λ is the decay constant (4.62E-7 yr^{-1}), and ρ is the rock or soil density (g cm^{-3}).

2.3.3 Scaling Factors

The scaling process for ^{10}Be is similar to that covered above for *in-situ* ^{36}Cl production. The EL correction is a cubic polynomial ($y = a + bx + cx^2 + dx^3$) where x is the elevation above sea level in km and y is the scaling factor (Lal 1991). The values for a,b,c and d for ^{10}Be at various latitudes are in Table 2-3. These polynomials are for production of ^{10}Be in quartz due to spallation and muon capture.

TABLE 2-3 Production rates of ^{10}Be in quartz (atoms $^{10}Be)(gSiO_2)^{-1}$ yr^{-1} from Lal, 1991

Latitude	a	B	C	d
0°	3.511	2.547	0.95125	0.18608
10°	3.360	2.522	1.0668	0.18830
20°	4.0607	2.734	1.2673	0.22529
30°	4.994	3.904	0.9739	0.42671
40°	5.594	4.946	1.3817	0.53176
50°	6.064	5.715	1.6473	0.68684
60-90°	5.994	6.018	1.7045	0.71184

3. METHODOLOGY

3.1 SAMPLING

The Bishop Creek moraines were chosen for this study due to the abundance of information already gathered at the site. The geomorphology, stratigraphy, and chronology of the moraines have been examined by numerous authors (Phillips et al. 1998; Sharp and Birman 1963; Zreda and Phillips 1994a). Such an extensive background allowed this project to target previously mapped and dated moraines for the erosion study.

Soil and rock samples were collected on ten moraines whose ages range from 17 ky to 150 ky. On each surface, a shallow (50 cm) pit was dug at the horizontal moraine crest. Samples were taken at depths: 0-5 cm, 20-25 cm, and 40-45 cm. Approximately 1 kg of soil and rock were collected at each depth. Gravel clasts in excess of 4-5 cm in diameter and roots were removed from the grab sample.

In addition, on three moraines, soil pits 1.5 m deep were dug for atmospheric ^{10}Be and *in-situ* ^{36}Cl studies. The depth was sufficient to account for most of the meteoric ^{10}Be in the soil profile. Samples were collected from nine intervals, each about 15 cm thick throughout the pit profile.

The samples were sealed in large plastic bags, then wrapped in plastic wrap and duct tape to ensure the integrity of the samples during shipping.

3.2 SAMPLE PREPARATION

The samples were dried at 70°C and sieved to separate three fractions: <0.25 mm, 0.25 to 1 mm, and 1 to 2 mm. Anything coarser than 2 mm was ground using a roller mill until the previous three size fractions were achieved.

For the *in-situ* studies using ^{36}Cl and ^{10}Be, the 0.25 to 1 mm fraction was leached in a 5% nitric acid bath to remove organics and any meteoric component. The samples were then dried again at 60 °C. From here the ^{10}Be and ^{36}Cl sample preparations are different.

3.3 TOTAL CHLORINE DETERMINATION

Total chlorine content of the samples was measured using diffusion cells and a chloride ion-specific electrode (Aruscavage and Campbell 1983; Bebeshko and Nesterina 1993). The sample was decomposed in a mixture of HF and H_2SO_4 in the outer chamber of a teflon diffusion cell. Chloride was transferred to the gas phase and then captured by the reducing solution in the inner chamber of the cell. The chloride concentration was measured by the electrode in the reducing solution. For each group of samples, three or four chloride standards were used to develop a calibration curve. This procedure was replicated a minimum of three times until total Cl values were within 15% of each other. Details of the procedure are found in Appendix A.

3.4 SEPARATION OF CHLORINE

The samples for ^{36}Cl were prepared using the procedure outlined by Zreda and Phillips (Zreda et al. 1991), in which the sample is dissolved in hot hydrofluoric and nitric acids in the presence of silver nitrate. In a series of acid/base reactions, chlorine is purified of sulfur, precipitated as AgCl and loaded into targets for use at PRIME Lab to determine $^{36}Cl/Cl$ (Elmore and Sharma 1997). Details of the procedure are in Appendix B.

3.5 SEPARATION OF METEORIC AND *IN-SITU* BERYLLIUM

Studies of *in-situ* ^{10}Be require the separation of pure quartz before BeO targets can be produced by a chromatographic procedure. The isolation of quartz is achieved by placing the sample in a 1% HF solution (5 to 15 g sample/ 2L of acid solution) for several hours in a hot (80 °C) sonicating water bath (Kohl and Nishiizumi 1992). The sample is then rinsed with deionized water and the process is repeated 3-5 times until only quartz remains. The pure quartz is then rinsed with deionized water until neutralized and dried at 60 °C. Higher extraction efficiency may be achieved by using a Frantz magnetic separator to separate heavier mafic minerals prior to chemical treatments.

Targets for meteoric and *in-situ* ^{10}Be samples were produced in the laboratory of Dr. Devendra Lal at Scripps Institution of Oceanography. The quartz separates for *in-situ* ^{10}Be were dissolved in concentrated HF and purified in a series of acid/base reactions and perchloric fumings prior to running the acidified solution in columns filled with ion-

specific resin (AG50W-X8 Bio-Rad Resin). $Be(OH)_2$ was precipitated into a gel from the solution that comes out of the first three pore volumes of the column, using ammonium hydroxide. This gel was then dried slowly to a powder and combusted in a furnace at 950 °C for half an hour to convert the sample to BeO that could then be loaded into targets. Specifics of the extraction technique are in Appendix C.

The technique for the meteoric ^{10}Be samples was slightly more involved in the initial purification stages. The <0.25 mm mesh size sample was purified using EDTA, chloroform and acetyl acetone in a heavy liquid separation prior to running the samples through the columns. After the columns, the procedure was identical to that outlined above for the *in-situ* ^{10}Be samples. A detailed description of the procedure is in Appendix D.

3.6 ISOTOPIC AND GEOCHEMICAL ANALYSIS

Chlorine-36 and ^{10}Be were analyzed by accelerator mass spectrometry at Purdue University. Chemical composition of the samples was determined by X-ray Assay Labs (XRAL) in Ontario, Canada. To determine major and selected trace elements (B, Gd, U, and Th) in the rocks, a few grams of the nitric acid leached, 0.25 to 1mm size fraction was powdered in a tungsten ball mill and sent for analysis.

4. ESTIMATING EROSION RATE AND EXPOSURE AGE

4.1 ESTIMATING EROSION RATE AND EXPOSURE AGE USING *IN-SITU* ^{36}Cl

In 1990, Fred Phillips proposed using the accumulation of ^{36}Cl in moraine boulders to determine surface exposure ages (Phillips et al. 1990). By sampling boulders on moraine crests near Bishop Creek, California, Phillips has developed a glacial chronology of the moraines (Phillips et al. 1998). The dating of surfaces using boulders, however, requires the sampling of many boulders on each moraine to obtain accurate exposure ages (Zreda and Phillips 1994a) because the boulders were found to have a range of exposure histories. It was determined that only the oldest boulders had been exposed since the glacial retreat and younger ages were due to partial shielding and subsequent exposure (Zreda and Phillips 1994b).

In the early 1990's, Zreda and Phillips used granitic boulders from the moraine crests in Bishop Creek to assess ^{36}Cl surface exposure ages. Samples taken from multiple boulders on each moraine yielded a range of ages (Zreda and Phillips 1994a). This range was small for young moraines, but for older moraines (150 ky) the data points were widely scattered (Zreda and Phillips 1994a). Because of this variability many boulders are required to determine the surface age.

Zreda and Phillips (1994a) interpreted the oldest ages to be the true ages of the surfaces. The authors proposed that some of the boulders now completely exposed on the crests might have in been buried by overlying soil that has since been removed leaving the boulder now fully exposed. Boulders that were exposed at the surface when the glacier retreated have the greatest accumulation of ^{36}Cl and represent the true age of the

moraine. A model of gradual exposure of the boulders was developed to explain the variability in ^{36}Cl ages (Zreda and Phillips 1994a) (Fig. 4-1).

A chronology of the moraines in Bishop Creek has been developed using ^{36}Cl in boulders (Phillips et al. 1998). The moraines sampled in this study are part of the Tahoe and Tioga terminal complexes described by Phillips (Phillips et al. 1998), and are illustrated in Figure 4-2. The series of moraines consists of terminal and lateral moraines nested together indicating multiple pulses of glacial activity. The Tungsten Hills moraines are a series of large lateral moraines that channeled subsequent smaller glaciers down what is now Sand Canyon. The Younger and Older Bishop, Coyote and Younger Tungsten Hills moraines are geomorphically distinct but all have been deposited in the interval 130 to 160 ky and do not exhibit any significant difference in ^{36}Cl age (Phillips et al. 1998). The recessional Younger Buttermilk (also known as Older Sand Canyon) is slightly younger (120-145 ky) (Phillips et al. 1998). The retreat of the Sand Canyon glacier during earliest Tioga, 25 to 30,000 years ago left three small terminal moraines in the canyon. The youngest moraine in the Bishop Creek Terminal complex is the Little Egypt lateral moraine and is considered to be 18 to 20,000 years old. The moraine ages (Phillips et al. 1998), and the corresponding sample numbers for this study using soils are summarized in Table 4-1.

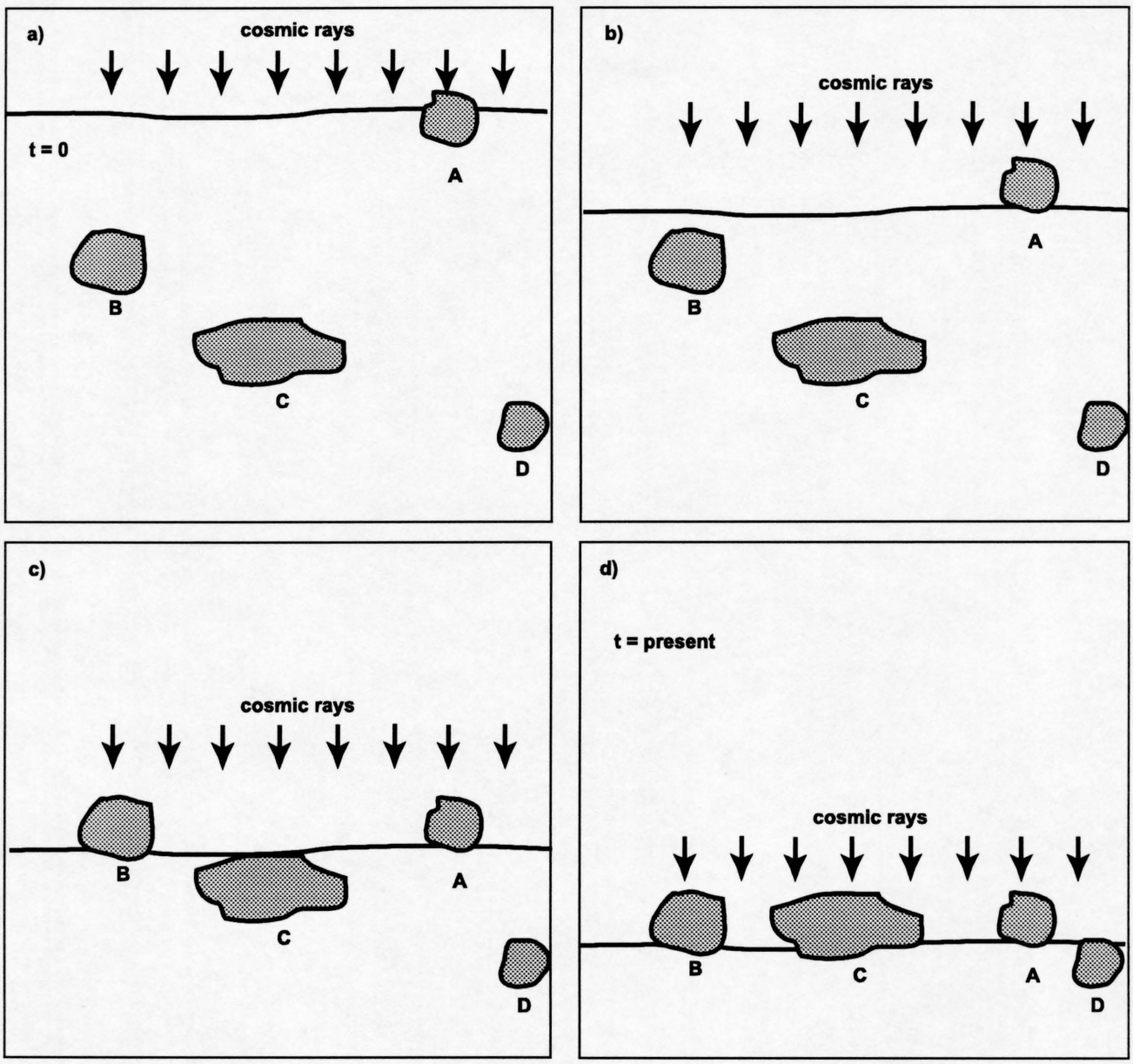

FIGURE 4-1 Gradual exposure model for moraine boulders (Zreda, et al., 1994). At t = 0 only boulder A is exposed (a). Through time the land surface is lowered (b and c) and new boulders are exposed. Today (d) all boulders are exposed, but only boulder A will yield the true exposure age because it has been exposed for the entire time since the moraine formation.

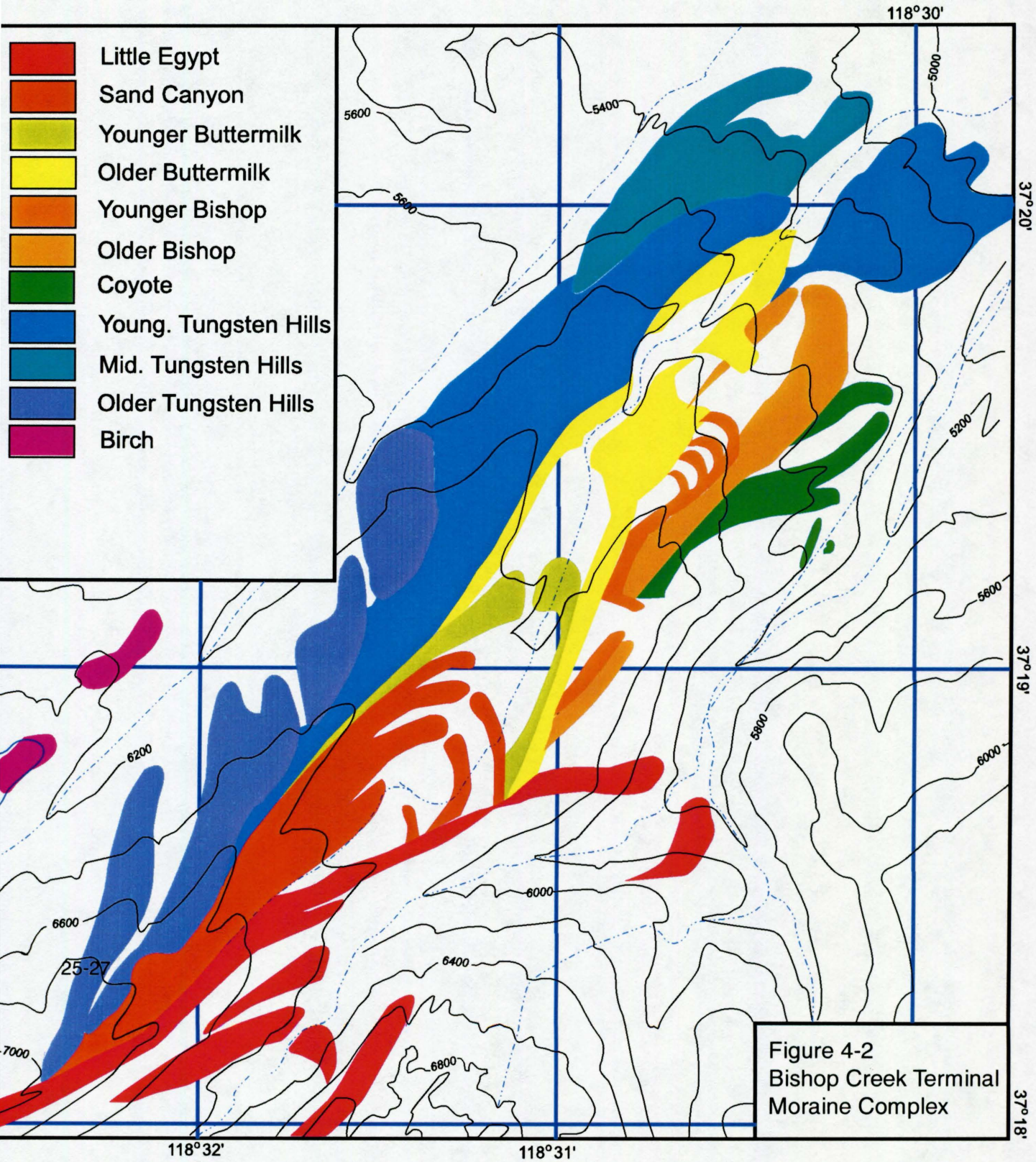

Figure 4-2
Bishop Creek Terminal
Moraine Complex

TABLE 4-1 Moraine age (from Phillips et al. 1998)

Moraine Name	Moraine Age	Soil Sample Numbers
Little Egypt	18 to 20 ky.	BPCR96-31,32,33
Sand Canyon	25 to 30 ky.	BPCR96-13,14,15
Younger Buttermilk (a.k.a. Older Sand Canyon)	120 to 145 ky.	BPCR96-10,11,12
Younger Bishop	130 to 160 ky.	BPCR96-19,20,21
Older Bishop	130 to 160 ky.	BPCR96-28,29,30
Coyote	130 to 160 ky.	BPCR96-16,17,18,19
Younger Tungsten Hills	130 to 160 ky.	BPCR96-1,2,3,4,5,6,37,38,39
Older Tungsten Hills	140 to 220 ky.	BPCR96-7,8,9
Birch	>200 ky.	BPCR96-34,35,36

This study uses the exposure ages reported by Phillips (Phillips et al. 1998), and the *in-situ* accumulation of ^{36}Cl in moraine matrix on the moraine crests to evaluate the lowering rates of the surfaces. Because exposure age (t) and erosion rate (ε) are unknowns in the ^{36}Cl build-up equation, the accumulation of ^{36}Cl alone in soils cannot be used to determine both variables.

In order to simultaneously calculate (t) and (ε) from the same sample, the isotopes of ^{36}Cl and ^{10}Be, with different half-lives (301 ky and 1,500 ky, respectively), were used together. This allowed for an independent check of exposure ages previously reported from the boulder study. Results of this study are found in sections 4.2 and 4.3.

4.1.1 In-situ ^{36}Cl *in soil*

Shallow soil pits were dug on the crests of nine Bishop Creek moraines near the boulder sampling locations of Phillips and Zreda (Phillips et al. 1998; Zreda and Phillips 1994b). Three pits were dug at different locations on the crest of the Younger Tungsten Hills moraine. Sample locations are illustrated in Figure 4-3.

Each of the shallow pits was 45-50 cm in depth. With the exception of the Birch moraine (>200ky), none of the moraine surfaces have a well developed soil horizon. In each pit the material ranged from silt to large cobbles. The older surfaces had greater chemical and physical degradation of the buried granitic rock than the younger surfaces.

The computer program CHLOE (Phillips and Plummer 1996) has been used to calculate moraine lowering rates assuming the exposure age previously determined (Phillips and Plummer 1996; Phillips et al. 1998) from boulders. For each soil sample, a bulk density of 2.0 g/cm^3 was assumed.

The calculated erosion rates are shown in Figure 4-4. The younger surfaces, such as the Little Egypt (18-20 ky) and Sand Canyon (25-30 ky), have the greatest errors of 19 and 13 percent respectively. This is an expected result from the low $^{36}Cl/Cl$ values measured in young samples. All other erosion rates have less than 10 percent error, typically 3 to 5 percent.

Erosion rates range from 18.4 to 63.4 mm/ky with most values being in the range from 35 to 50 mm/ky. The value for the Younger Tungsten Hills #4 is anomalously high compared to the other samples from the same moraine and is probably in error. Further explanation is given in Section 4.3.

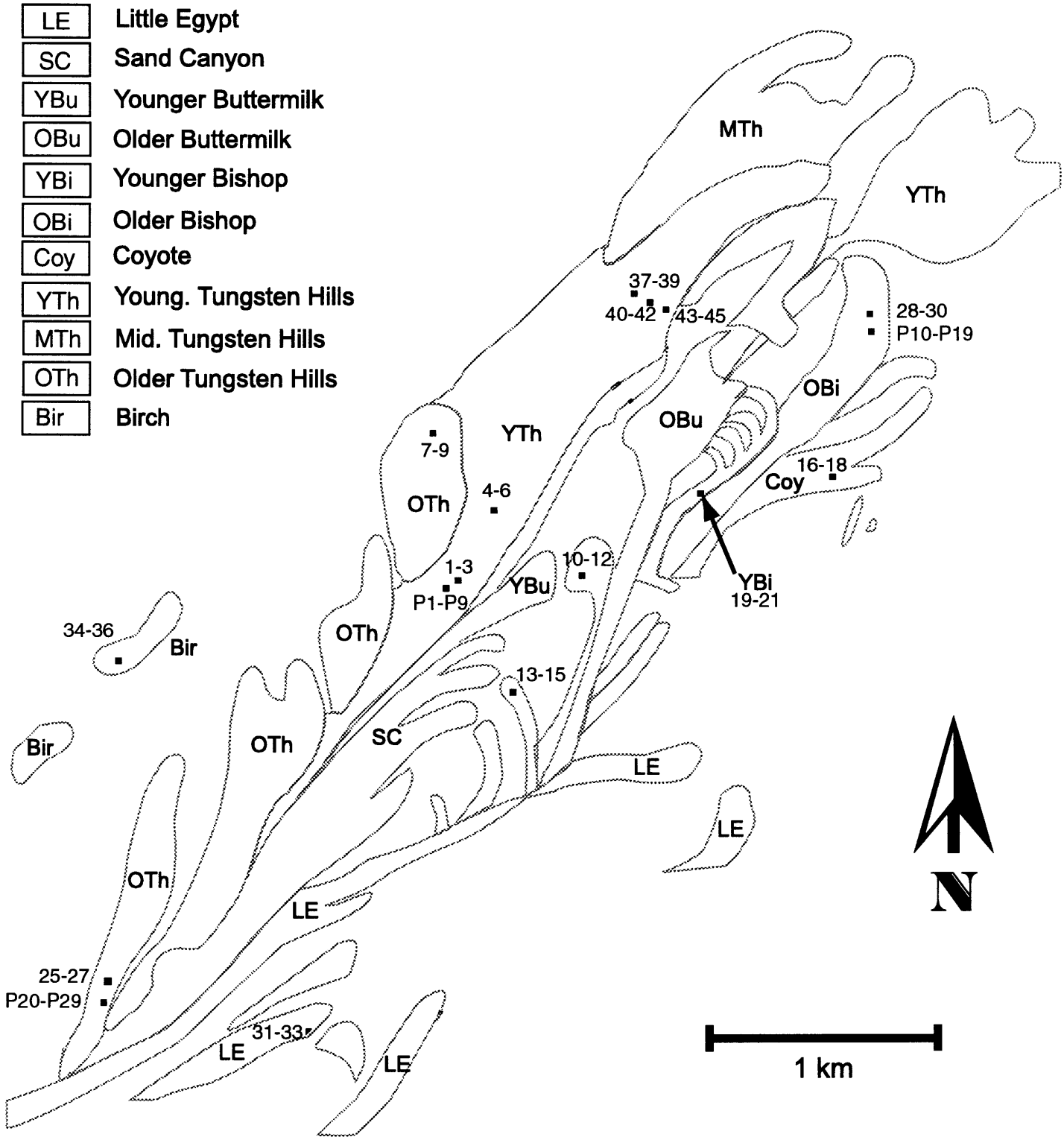

FIGURE 4-3 Moraine Outlines and Sample Locations

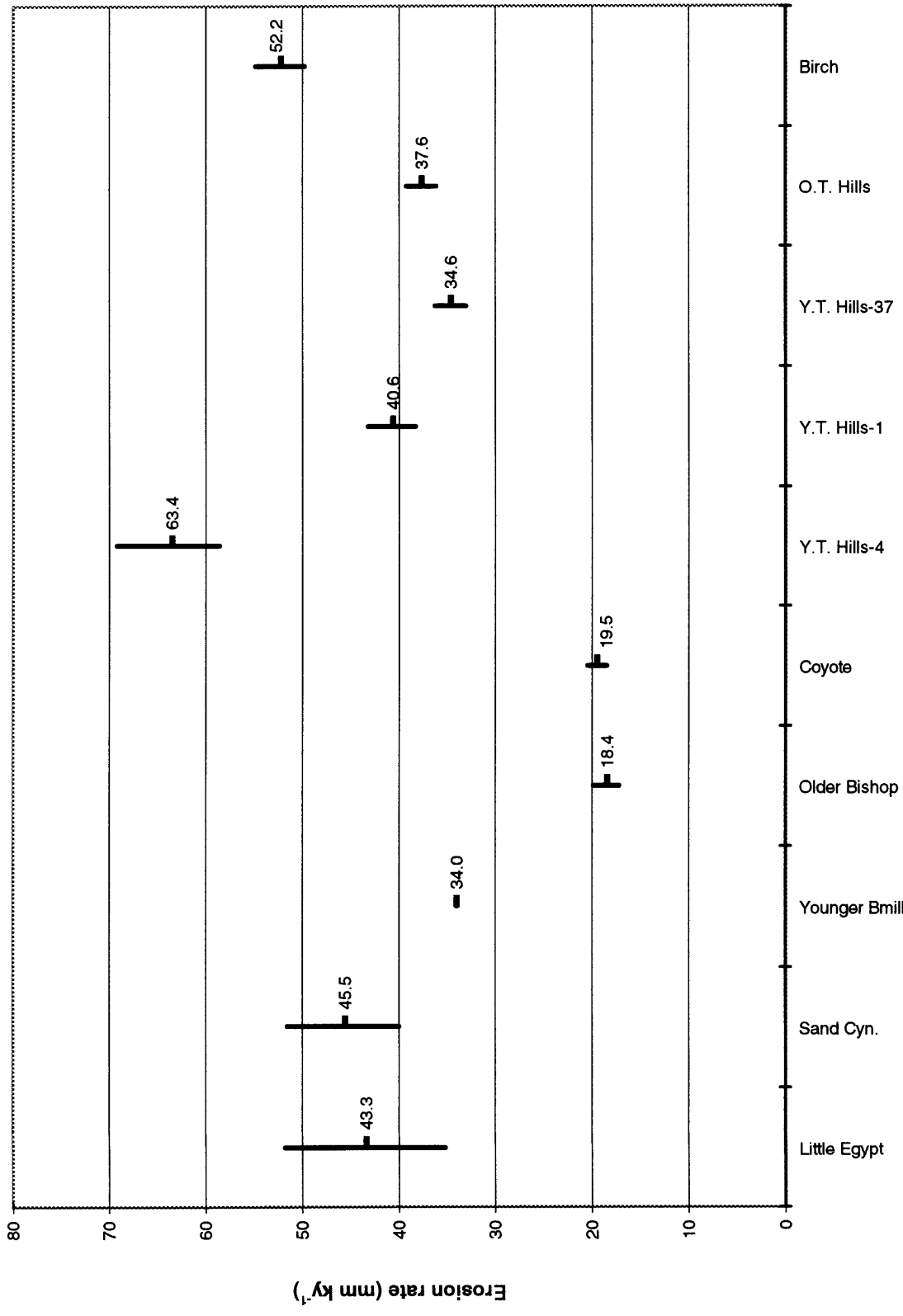

FIGURE 4-4 Erosion rates from *in-situ* ^{36}Cl

4.2 ESTIMATING EROSION RATE AND EXPOSURE AGE USING *IN-SITU* AND METEORIC ^{10}Be IN SOIL

4.2.1 In-situ ^{10}*Be*

Splits of ^{36}Cl samples were used for ^{10}Be analyses. Pure quartz was separated from the samples using a Frantz magnetic separator and an ultrasonic acid bath. Beryllium was extracted from the quartz and purified in Dr. Devendra Lal's laboratory at Scripps Institution of Oceanography. Details of the methods can be found in Section 3.5 and Appendix C.

The accumulation of ^{10}Be is calculated using the following equation (Nishiizumi et al., 1991):

$$N = P/(\lambda + \rho\varepsilon/L)\,(1 - e^{-(\lambda + \rho\varepsilon/L)t})$$

where N is the measured ^{10}Be concentration (atoms (g SiO_2)$^{-1}$), P is the production rate (atoms (g SiO_2)$^{-1}$ yr^{-1}), t is the exposure time (yr), ε is the erosion rate (cm yr^{-1}), L is the attenuation length (160 g cm^{-2}), and ρ is the bulk density (2.0g cm^{-3}). The production rate is aproximately 23 atoms (g SiO_2)$^{-1}$ yr^{-1} based on 5.6 atoms (g SiO_2)$^{-1}$ yr^{-1} (Nishiizumi et al. 1989) at sea level and 37°N latitude, and an ELD scaling factor of 4.11 calculated using Lal (1991).

This equation was solved for erosion rate (ε) with a known range of ages (t) determined previously (Phillips et al. 1998). Figure 4-5 illustrates the range of erosion

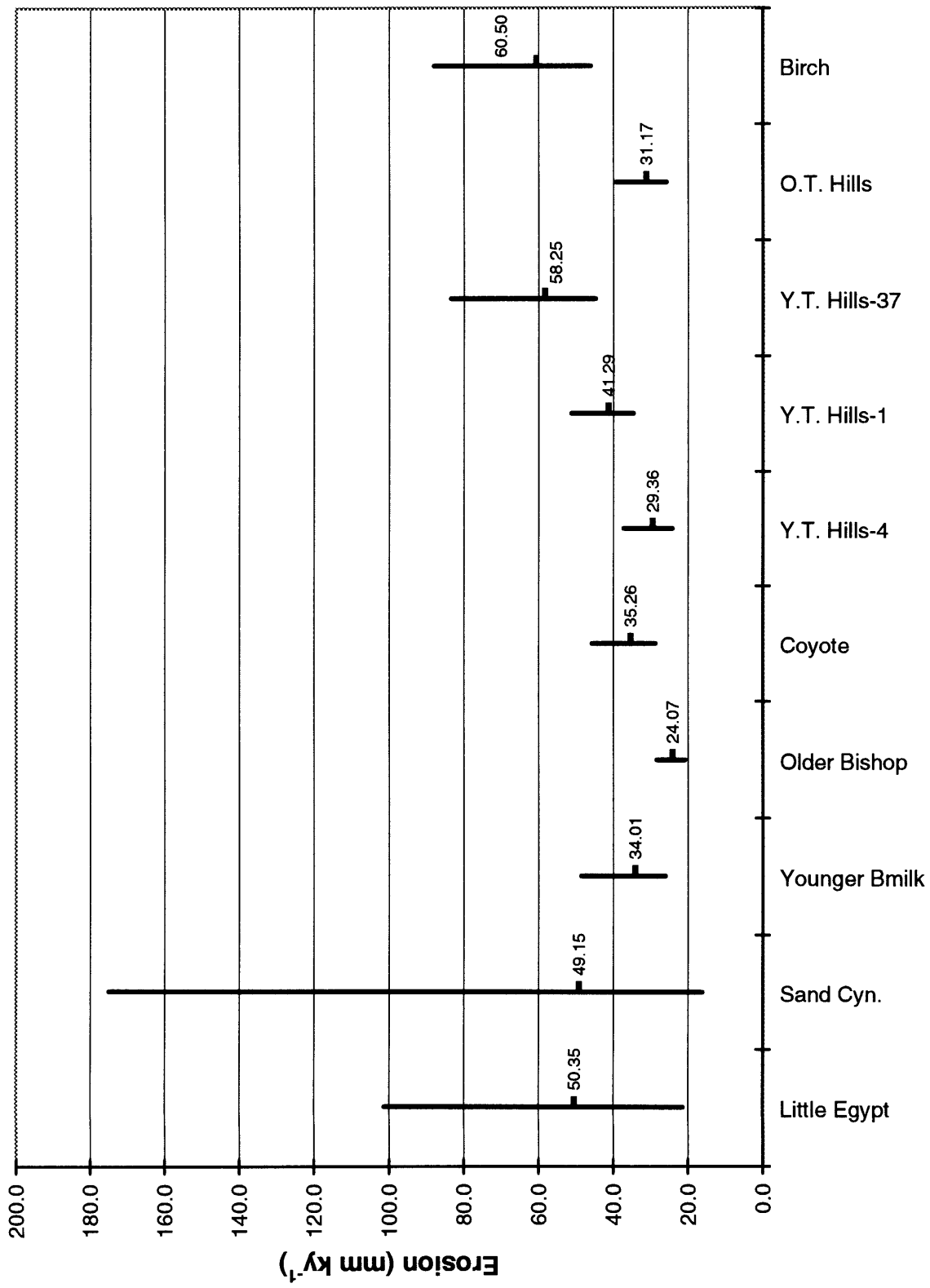

FIGURE 4-5 Erosion rates from *in-situ* ^{10}Be

rates calculated from the accumulation of *in-situ* ^{10}Be. Calculated erosion rates range from 24.1 to 60.5 mm/ky. The uncertainties for the youngest samples (<30 ky) are larger than for the older samples. These large errors can be attributed to an insufficient time for measurable buildup.

The variability in erosion rate seen in the three Younger Tungsten Hills samples implies some variability depending upon location on the moraine. Variations in moraine geometry, soil matrix or rock composition may contribute to such localized effects.

The Birch moraine is the most weathered moraine sampled and yields a high erosion rate. Though the topographic relief of the Birch moraine is minimal compared to other moraines, the excessive chemical alteration of the cobbles in the matrix makes the moraine increasingly susceptible to high erosion rates. The age of the moraine is curently estimated to be > 200 ky. Since this is a minimum age of the moraine, the erosion rate calculated is therefore a maximum, which can account for the comparatively high erosion rate.

4.2.2 Meteoric ^{10}Be

The accumulation of meteoric ^{10}Be in soils has been used with varying degrees of success to determine landform ages (Barg 1992; McHargue and Damon 1991; Monaghan et al. 1983) and erosion rates (Monaghan et al. 1986; Monaghan and Elmore 1994; Pavich et al. 1986). Meteoric ^{10}Be in soils is much more abundant than *in-situ* ^{10}Be, which allows for more consistent AMS measurements and smaller analytical errors.

Using meteoric ^{10}Be with one of the *in-situ* produced nuclides, both erosion rates (ε) and exposure age (t) can be obtained.

For the purpose of this study, soil pits 1.5 to 2 meters deep were dug in the Younger Tungsten Hills (130-160 ky), Older Bishop (130-160ky), and Older Tungsten Hills (140-220 ky) moraine crests. The measured $^{10}Be/Be$ and atoms of $^{10}Be/g$ are reported in Table 4-2 and the profile is shown in Figure 4-6.

As discussed in Section 2.3.1, the equation used for evaluating erosional loss of a portion of the ^{10}Be inventory in a soil profile is from Pavich (1986):

$$N = \frac{(q - \varepsilon m)}{\lambda}\left(1 - e^{-\lambda t}\right) \qquad (1)$$

where N is the measured ^{10}Be inventory [atoms $(g\ SiO_2)^{-1}$], m is the concentration of ^{10}Be in the surface layer [atoms $(g\ SiO_2)^{-1}$], λ is the decay constant for ^{10}Be ($4.62 \times 10^{-7}\ yr^{-1}$), t is the age of the surface from the ^{36}Cl boulder study [yr], q is the deposition rate for ^{10}Be (atoms $cm^{-2}\ yr^{-1}$), and ε is the erosion rate ($g\ cm^{-2}\ yr^{-1}$). A q value of 0.52×10^6 atoms $cm^{-2}\ yr^{-1}$ has been reported as a good approximation for temperate latitudes and rainfall similar to that in California (Monaghan et al. 1983; Pavich et al. 1986).

Pavich (1986) used equation 1 to determine a "predicted inventory" by assuming exposure age and an erosion rate of 3×10^{-4} g $cm^{-2}\ yr^{-1}$. This value was then compared to the "expected inventory":

$$N = q\,(1\text{-}e^{-\lambda t})/\lambda \qquad (2)$$

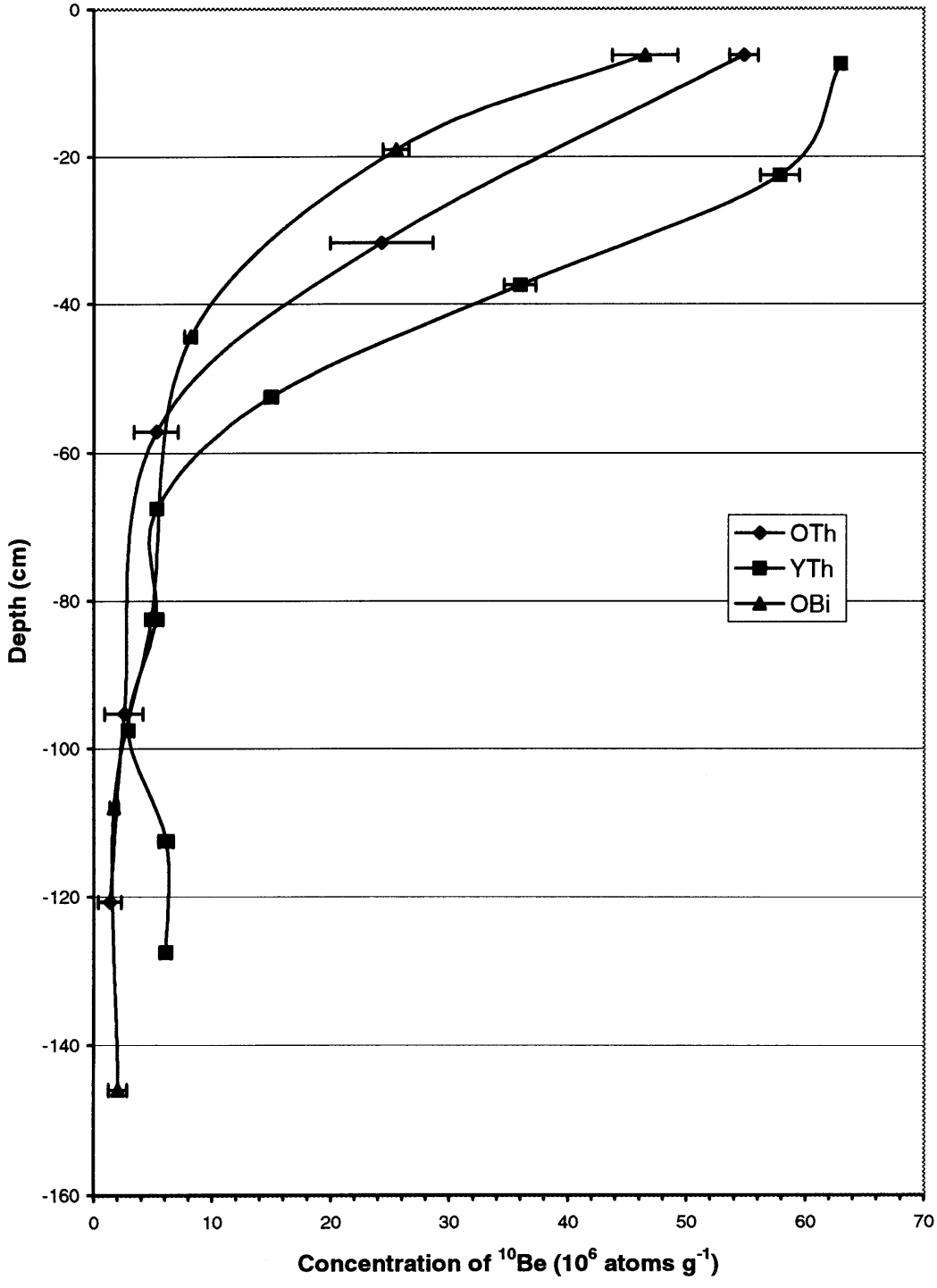

FIGURE 4-6 Meteoric 10Be profile

TABLE 4-2 Meteoric ^{10}Be from deep soil pits

Sample Number	Depth (cm)	$^{10}Be/^{9}Be$	Atoms $^{10}Be/g$ ($x10^{6}$)
Younger Tungsten Hills			
BPCR96 P-1	0-15	3340 ± 13	63 ± 0.2
BPCR96 P-2	15-30	3180 ± 90	58 ± 1.6
BPCR96 P-3	30-45	1900 ± 70	36 ± 1.3
BPCR96 P-4	45-60	798 ± 29	15 ± 0.5
BPCR96 P-5	60-75	277 ± 16	5 ± 0.3
BPCR96 P-6	75-90	140 ± 17	5 ± 0.6
BPCR96 P-7	90-105	79 ± 12	3 ± 0.4
BPCR96 P-8	105-120	167 ± 17	6 ± 0.6
BPCR96 P-9	120-135	160 ± 13	6 ± 0.5
Older Bishop			
BPCR96 P-10	0-12	1350 ± 80	47 ± 2.8
BPCR96 P-11	12-25	668 ± 29	26 ± 1.1
BPCR96 P-13	38-50	224 ± 14	8 ± 0.5
BPCR96 P-15	75-89	131 ± 13	5 ± 0.5
BPCR96 P-17	102-114	47 ± 10	2 ± 0.4
BPCR96 P-19	140-152	54 ± 21	2 ± 0.8
Older Tungsten Hills			
BPCR96 P-20	0-12	1510 ± 12	55 ± 0.4
BPCR96 P-22	25-38	651 ± 42	24 ± 1.6
BPCR96 P-24	50-63	140 ± 18	5 ± 0.7
BPCR96 P-27	89-102	70 ± 16	3 ± 0.6
BPCR96 P-29	115-127	38 ± 10	1 ± 0.4

If the expected and predicted inventory are in good agreement then the system is said to work well. If a discrepancy appeared, ^{10}Be was said to have been lost from the system by percolating vertically and lost to deeper soils, being physically removed down-slope, or by varying the average deposition rate through time.

Unlike ^{10}Be profiles of Pavich (1986) and Monaghan (1983), the profiles from the Bishop Creek moraines indicate the greatest accumulation in the upper 40 cm, with over 90% of the total inventory occurring in the upper 1 m of the profile (Fig. 4-6). Pavich reported significant amounts of ^{10}Be down to 3 and 4 m depths (Pavich et al. 1986) and the greatest accumulation of ^{10}Be in the 50 to 100 cm zone. This would seem to indicate that the Bishop Creek Moraines are retaining more ^{10}Be in the upper soil and not losing ^{10}Be to lower zones.

For the purpose of this study, it was assumed that erosion was the only significant contributing factor to the depletion of the measured ^{10}Be inventory. Equation 1 can be solved for erosion rate (ε) if we assume that the production rate (q) and the exposure age (t) are known (Equation 3).

$$\varepsilon = \frac{N\lambda}{-m\left(1 - e^{-\lambda t}\right)} + \frac{q}{m} \qquad (3)$$

As a first estimation, the production rate (q) of 0.52 x 10^6 atoms cm^{-2} yr^{-1} (Pavich et al. 1986) and the exposure ages (t) from the boulder study were used to calculate erosion rates. For all calculations, a density of 2.0 g cm^{-3} has been assumed for

the well graded moraine material. Results of the meteoric ^{10}Be erosion rates are found in Table 4-3.

TABLE 4-3 Calculated erosion rates from meteoric ^{10}Be

Moraine	Surface concentration m (10^6 g^{-1})	Calculated erosion rate (mm ky^{-1})	Error +	Error -
Younger Tungsten Hills	63 ± 0.2	41.3	0.1	0.2
Older Bishop	47 ± 2.8	55.9	3.6	3.2
Older Tungsten Hills	55 ± 0.4	47.4	0.3	0.4

The erosion rates using meteoric ^{10}Be range from 41 mm ky^{-1} (8.26 x 10^{-3} g cm^{-2} yr^{-1}) to 56 mm ky^{-1} (1.12 x 10^{-2} g cm^{-2} yr^{-1}). These values are in good agreement with values from the *in-situ* ^{10}Be and *in-situ* ^{36}Cl techniques. Section 4.4 compares the results of the three systems.

4.3 SENSITIVITY ANALYSIS

The erosion rate determined by equation (3) is driven almost entirely by the ratio of *q/m* and the other variables (N, t) are of little consequence. A sensitivity analysis of the Younger Tungsten Hills sample reveals a linear relationship between erosion rate and ^{10}Be production rate (q) (Fig. 4-7) while a ±40% change in total inventory (N) or surface age (t) has little effect on the calculated erosion rate. The surface ^{10}Be measurement (m) has an inverse relationship with the erosion rate with an asymptotic minimum erosion rate near 25 mm ky^{-1}.

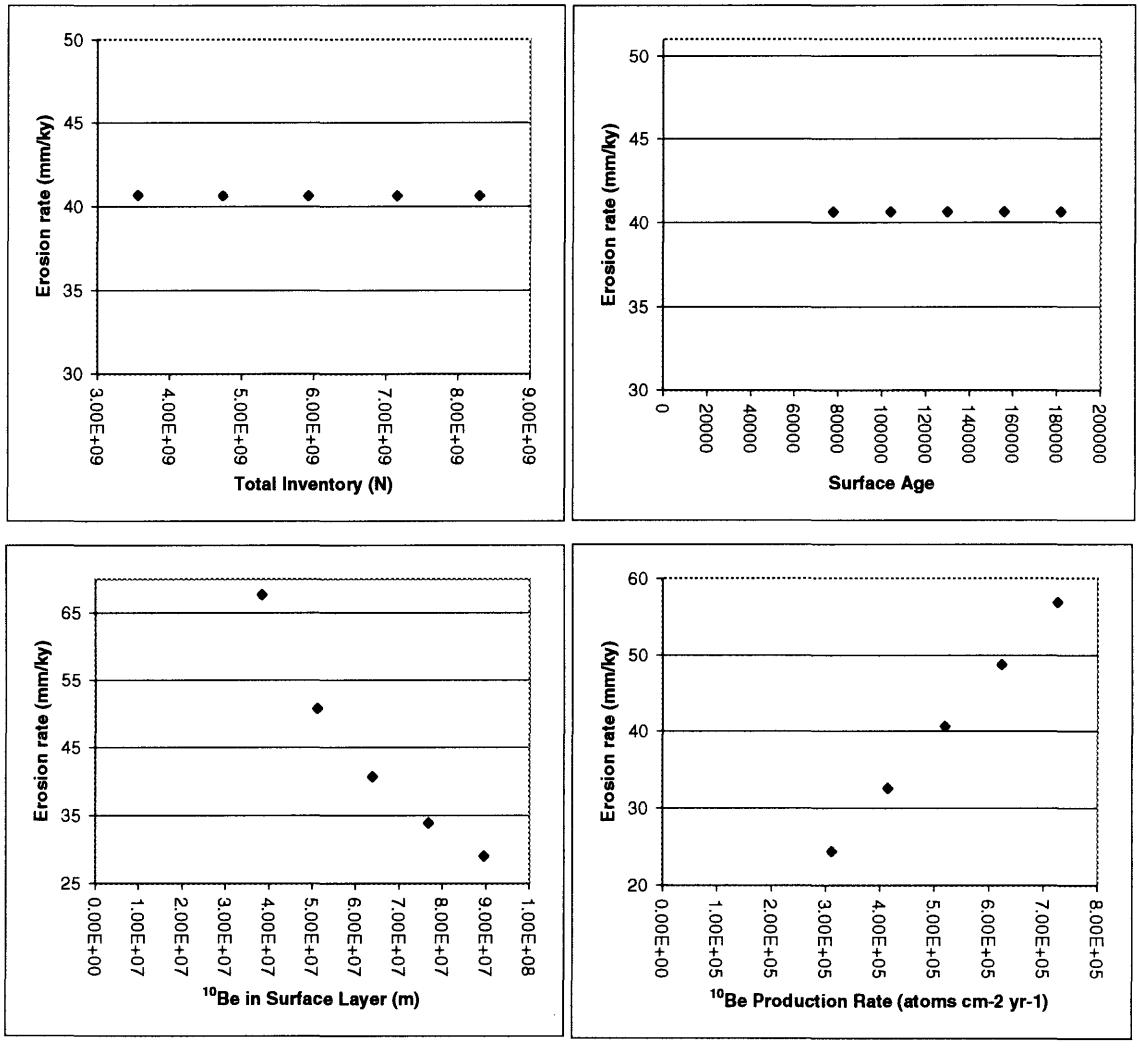

FIGURE 4-7 Sensitivity analysis of erosion rates from meteoric ^{10}Be Note: in each case the center value is the erosion rate computed for the Younger Tungsten Hills sample and the values to either side are ± 20% and 40% of that value for N, t, m and P.

4.4 COMPARISON OF EROSION RATES USING ^{10}Be AND ^{36}Cl

A comparison of erosion rates calculated from the two *in-situ* methods and from meteoric ^{10}Be shows a good correlation between systems (Table 4-4). Figure 4-8 is a visual representation of erosion rates calculated in the above sections using *in-situ* produced ^{10}Be and ^{36}Cl. With few exceptions, these two methods yield consistent results. For all moraines, the *in-situ* ^{10}Be has larger error bars than the samples analyzed using *in-situ* accumulated ^{36}Cl. The Little Egypt (18-20 ky) and Sand Canyon (25-30 ky) are too young for ^{10}Be to have accumulated to appreciable levels, which resulted in small BeO targets, and consequently, large error bars. The difference in calculated values, however, is typically within 5-10 mm ky^{-1}.

TABLE 4-4 Comparison of calculated erosion rates

Moraine	*In-situ* ^{36}Cl (mm ky^{-1})	*In-situ* ^{10}Be (mm ky^{-1})	Meteoric ^{10}Be (mm ky^{-1})
Little Egypt	43.3 (+8.4/-8.1)	50.4 (+50.9/-28.9)	
Sand Canyon	45.5 (+6.0/-5.5)	49.2 (+125.8/-33.0)	
Young. Buttermilk	Low sample yield	34.0 (+14.4/-8.0)	
Older Bishop	18.4 (+1.4/-1.3)	24.1 (+4.3/-3.3)	55.9 (+3.6/-3.2)
Coyote	19.5 (+1.0/-0.9)	35.3 (+10.3/-6.6)	
Y. Tung. Hills-4	63.4 (+5.7/-4.9)	29.4 (+7.8/-5.2)	
Y. Tung. Hills-1	40.6 (+2.6/-2.3)	41.3 (+9.8/-6.7)	41.3 (+0.1/-0.2)
Y. Tung. Hills-37	34.6 (+1.6/-1.5)	58.3 (+25.1/-13.5)	
O. Tung. Hills	37.6 (+1.6/-1.5)	31.2 (+8.0/-5.4)	47.4 (+0.3/-0.4)
Birch	52.2 (+2.7/-2.4)	60.5 (+27.4/-14.4)	

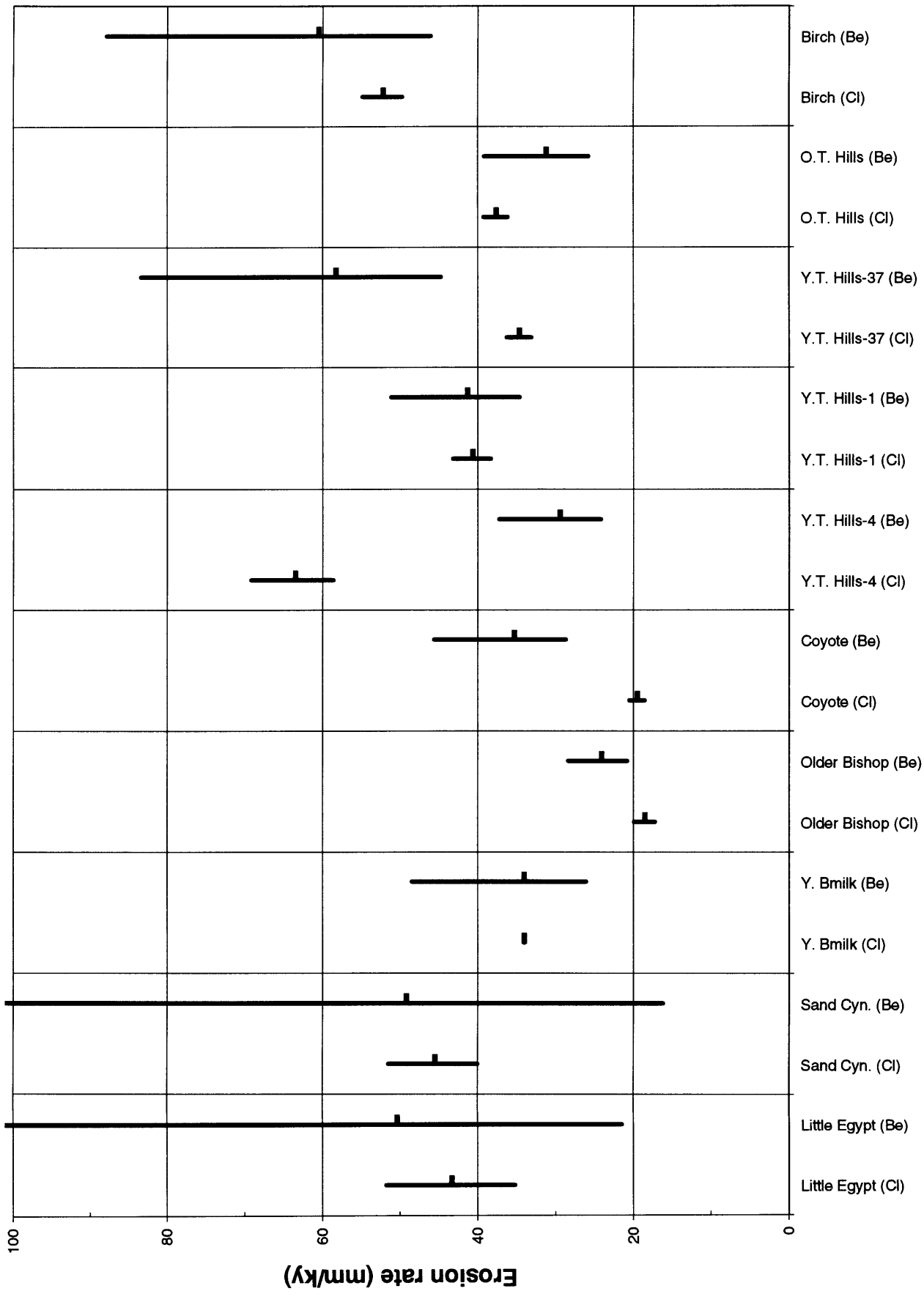

FIGURE 4-8 Comparison of calculated erosion rates using ^{36}Cl and ^{10}Be

Calculated erosion rates range from 18 to 63 mm ky^{-1}. The two youngest moraines (18-30 ky) have lowering rates of 45-47 mm ky^{-1}. The Younger Buttermilk (120-145ky) moraine has results only from the *in-situ* ^{10}Be due to unusually large errors recorded during AMS measurement of ^{36}Cl rendering that sample unusable. The single result of approximately 35 mm ky^{-1} is intermediate between the younger Sand Canyon moraine and the older group of moraines including the Older Bishop and Coyote moraines (both 130-160 ky) which have the lowest erosion rates of the Bishop moraines at approximately 18 to 25 mm ky^{-1}. The Younger Tungsten Hills moraine was sampled at 3 locations along the crest for *in-situ* ^{10}Be and ^{36}Cl and a deep pit was dug next to YTh-1 for meteoric ^{10}Be studies. The three sample sites indicate some variability in erosion rate at varying locations on the same moraine. The three values taken at YTh-1 agree very well with an erosion rate of approximately 41 mm ky^{-1}. Younger Tungsten Hills 4 and 37 have discrepancies between the ^{10}Be and ^{36}Cl values. In YTh-4, ^{10}Be underestimated erosion rate relative to ^{36}Cl, while this is reversed in YTh-37.

Sample YTh-37 may have over estimated the erosion rate in the ^{10}Be system because the sample was taken a third of the way down the slope. Beryllium's strong affinity for solid particles, particularly clays, (Brown et al. 1987; Brown et al. 1989; Monaghan and Elmore 1994; Monaghan et al. 1983; Pavich et al. 1984; Pavich et al. 1985) has made the isotope attractive for soil studies. The accumulation and immobilization of ^{10}Be in the upper lithosphere means that is unlikely to be mobilized by fluids passing through it (Gu et al. 1996; Pavich et al. 1986; Pavich et al. 1985). Physical

removal of clay particles and transport downslope could deplete the ^{10}Be in hill-top profiles while forming thicker deposits of clays containing some inherited ^{10}Be on the slopes (Monaghan and Elmore 1994). This may cause the ^{10}Be profiles to be thicker but of lower concentration which could manifest itself as either an erosion rate that is too high or as a surface that is too young. On the moraine slopes, the beryllium may be more susceptible to the effects of erosion and physical removal than the chlorine is. A suggestion for further study of the effects of hillslope processes on the chlorine and beryllium systems is presented in the recommendation section.

5. ESTIMATING DEPOSITION RATE FOR METEORIC ^{10}Be

In section 4.2.2 meteoric ^{10}Be was used to determine the erosion rates for three moraines at Bishop Creek. This required knowing the exposure age (t) and the deposition rate of meteoric ^{10}Be (q). In the earlier sections, a value of 0.52×10^6 atoms cm^{-2} yr^{-1} was adopted from previous work (Monaghan et al,. 1986; Monaghan et al., 1983 who considered this value to be valid for arid parts of California. Because Bishop is at a similar latitude and has similar precipitation rate, this value was used as a first approximation for all calculations.

Assuming the erosion rate (ε) calculated using *in-situ* ^{36}Cl and ^{10}Be in soils, and the exposure age (t) from the boulder study, we may obtain an independent estimate of the ^{10}Be production rates specific to the Bishop field site, averaged over the age of the individual landform. Pavich's equation (Equation 1) for meteoric ^{10}Be inventory (N) may be solved for the deposition rate as follows:

$$q = \frac{N\lambda}{\left(1 - e^{-\lambda t}\right)} + \varepsilon m \qquad (4)$$

In this equation, for landforms whose ages are older than ~ 100 ky, the denominator has a negligible effect in the overall calculation. Because N is the inventory from the measured value of ^{10}Be, and λ is a constant, the computation of deposition rate is highly dependent upon the erosion rate (ε) and the ^{10}Be in the surface layer (m).

The average erosion rate used in this computation was calculated using the maximum and minimum erosion rates obtained once errors had been added for both *in-*

situ systems. The range of erosion rates (ε) used to calculate a range of meteoric ^{10}Be production rates is listed in Table 5-1.

The values for the ^{10}Be in the surface layer (m) were measured from samples taken from the top 15 cm of the deep soil pits. This sample represents a chemical average of the top 15 cm. The value immediately at the surface was computed by matching best fit curves to the top 40 cm of the ^{10}Be profile (Figure 4-6) and extrapolating to the surface. The estimated surface values of ^{10}Be are shown in Table 5-1.

Using the values for m and ε described above, the mean ^{10}Be deposition rate is $0.46 \pm 0.16 \times 10^6$ atoms cm^{-2} yr^{-1}. These values compare well with the previous estimate of 0.52×10^6 atoms cm^{-2} yr^{-1} for northern California (Monaghan et al. 1983). The data in this study are limited to three soil profiles, but these preliminary results show promise for further study of ^{10}Be deposition in arid areas.

TABLE 5-1 Estimation of meteoric ^{10}Be deposition rate

Surface	Age (ky)	Surface conc. M (10^7 g^{-1})	*In-situ* calculated. erosion rate (mm ky^{-1})	Meteoric ^{10}Be prod. Rate (q) (10^6 atoms cm^{-2} yr^{-1})
Yth	130	6.59 ± 0.04	44.6 ±13.4	0.64± 0.18
Yth	160	6.59 ± 0.04	44.6 ±13.4	0.63 ± 0.18
Obi	130	6.16 ± 0.28	21.6 ± 4.8	0.29 ± 0.07
Obi	160	6.16 ± 0.28	21.6 ± 4.8	0.28 ± 0.07
Oth	140	6.26 ± 0.11	35.1 ± 6.4	0.46 ± 0.09
Oth	220	6.26 ± 0.11	35.1 ± 6.4	0.45 ± 0.09

6. SUMMARY

The combination of *in-situ* ^{36}Cl and ^{10}Be allowed for the simultaneous calculation of landform age and erosion rate. The age values obtained from this study agreed well with previous estimates using ^{36}Cl accumulation in boulders and required only a fraction of the number of total samples.

Erosion rates were calculated using the accumulation of *in-situ* ^{36}Cl and ^{10}Be as well as meteoric ^{10}Be. Erosion rates for the Bishop Creek moraines ranged from 19 to 62 mm ky^{-1} with most values in the 30-45 mm ky^{-1} range. Chlorine-36 and meteoric ^{10}Be yielded small errors, typically less than 10% of the calculated erosion value. Measurements from *in-situ* accumulation of ^{10}Be had larger errors than the ^{36}Cl system, especially on young surfaces. The erosion rates calculated using *in-situ* ^{10}Be typically overestimated erosion rates by 10-20% compared to the same calculations using ^{36}Cl. This is could be accounted for by a 10 to 15% over-estimate of the ^{10}Be production rate.

The deposition rate (q) of meteoric ^{10}Be was examined in three deep pits in this study. The mean ^{10}Be production rate was calculated to be $0.46 \pm 0.16 \times 10^6$ atoms cm^{-2} yr^{-1} which agrees well with the estimate of 0.52×10^6 atoms cm^{-2} yr^{-1} (Monaghan et al. 1983; Pavich et al. 1986). A slightly lower production rate could bring the erosion rates using ^{10}Be and ^{36}Cl into an even closer agreement. These results encourage further study of meteoric ^{10}Be deposition rates.

7. RECOMMENDATIONS

In completing the work contained in this document, the author would like to make several recommendations for scientists conducting similar work. A suggestion for a related study to evaluate the influence of hillslope processes on cosmogenic isotope buildup in soils is also proposed.

7.1 RECOMMENDED PIT SAMPLING PLAN FOR ^{10}Be

Because of the high analytical cost of ^{10}Be samples, it may be possible to reduce the number of meteoric samples in third. In this study multiple samples were taken and evaluated for each 1.5 meter deep pit. In all cases, > 90% of the total inventory was recovered within the first 80 cm of pit depth. This would allow the total depth of the pits to be decreased from 1.6 or 1.75 meters to approximately 1.0 meter in this arid region hence, saving time in the field.

The two most important factors in calculating exposure age using meteoric ^{10}Be are the $^{10}Be/Be$ value found in the surface layer and the total inventory measured. As the greatest influence in the surface exposure age calculation is from the surface measurement, smaller intervals should be sampled in the top 15 cm to better define the true ^{10}Be content of the surface interval. The top two samples and bottom sample from the pit should be analyzed. Equal masses (10-20 g) of the intermediate samples could be combined to give an average sample. In this way, four samples could adequately define the ^{10}Be in the surface interval, the total inventory and whether the bottom sample was taken at a depth sufficient to account for the majority of accumulated ^{10}Be. Remaining

sample portions should be kept separate in case more detail becomes necessary. Evaluation of these four samples does not yield a detailed subsurface production curve, but it may be used for determining the total inventories with adequate precision at a significant saving of both time and money.

7.2 HILLSLOPE PROCESSES AND COSMOGENIC ISOTOPE ACCUMULATION

All samples in this study were collected from the stable crests of moraines. On the hillslopes, however, some of the inventory may have been inherited by physical removal of soils from the upper slopes and deposition on lower slopes. The meteoric component should be especially sensitive to this sort of transport because meteoric ^{10}Be sorbs more readily on fine grained material.

During the field work, shallow samples were collected on a transect perpendicular to the crest of the from the Younger Tungsten Hills moraine at the crest, a third of the way down, two thirds of the way down and at the bottom of the moraine. By taking a series of samples from a moraine with good age control the author was hoping to compare the results in the pits down-slope to assess the mobility of isotopes due to hillslope processes. With time and monetary constraints, this study was never done but could be a follow up study for another master's thesis project.

7.3 ^{10}Be PRODUCTION RATE

The three deep pits sampled for determining the meteoric ^{10}Be production rate yielded promising results, but greater sample numbers could make this a more definitive

study. The moraines in the Bishop Creek terminal complex provide an excellent opportunity to study production rates. The exposure ages are well known, and the arid environment has not caused excessive vertical mobility of the ^{10}Be. A dozen or more sample pits could be dug on moraines of varying ages allowing for estimates of time averaged ^{10}Be production rates. A couple weeks of field sampling and about a month of lab work could yield some very important estimates of production rate.

APPENDIX A

Total Chlorine Determination

Total Chlorine Determination

1. Clean the teflon diffusion cells using: 1) 1 L H_2SO_4 + 35 ml $K_2Cr_2O_7$; 2) deionized water; 3) 300 ml hot HNO_3 + 25 ml H_2O_2; 4) Mill-eq water

2. Once the cells have been cleaned, make sure that they are appropriately labeled and dry.

3. Make a sheet in the appropriate project notebook for total chlorine with the following headings:
   Cell#, Name, Mass Empty, Mass In, Mass Out, MV

4. Decide upon the appropriate standards to use 20, 40, 100 ppm etc. For samples with low chlorine content (<60 ppm) 4 standards may be necessary. Others may only require 2-3 standards per set of diffusion cells. Note: 2 sets of standards are necessary 1 set for cells 1-12, 1 set for 13-24

5. Make up reducing solution (for 24 cells) put in labeled reducing bottle
   12.0 g KOH + 0.6 g Na_2SO_3 + 64 g Mill-eq water

6. Make up oxidizing solution (for 24 cells) put in oxidizing bottle
   0.8 g MnO_4 + 11.2 g MilliQ water + 3.8 ml 50% H_2SO_4 + 64 ml HF

7. Place capped oxidizing and reducing solutions on orbital shaker at low speed to mix until needed

8. Measure and record the empty weight of all cells

9. Using designated pipets, pipet 0.200 +/- 0.01 g of solution standards (ie 100ppm...) into the outside of cells designated for standards

10. Add 0.200 +/- 0.01 g of powdered sample to the outer chamber of the cells and record mass.

11. Place cells under fume hood so that they are tilted slightly with sample/ standard on the upper side of the cell.

12. Measure 2.5 ml of reducing (clear) solution into the inner chamber of the diffusion cells

13. Measure 3.0 ml of oxidizing solution (purple) to the lower portion of the outer chamber of the diffusion cells making sure not to let the solution contact the sample

14. Close cells and place on shaker speed <200 for between 16-20 hours

15. Change solution in ion selective electrode and rinse electrode with mill-eq

16. Open the blank, pipette off solution from outer chamber using the designated garbage pipette

17. Weigh the cell, write down in Mass out column in table.

18. Put electrode in blank for 30 min. The bottom of the electrode should be fully imersed in the solution but should not touch the bottom of the diffusion cell. Record potential at beginning and end of this period.

19. Open diffusion cell and pipette off solution from outer chamber (one at a time).

20. Weigh each cell and calculate the mass of solution left in the cell

21. Rinse the electrode, shake off any droplets of water while covering the filling port on upper side of electrode

22. Place electrode into diffusion cell and press measure. If it beeps immediately, press measure again. It should take about 1 min to measure the sample and beep.

23. Record measurement of potential in mV column (make sure it is measuring in mV)

24. Rinse diffusion cell after use and put on CLEAN towel.

25. Repeat steps 19-24 for each diffusion cell

APPENDIX B

Chlorine Extraction Proceedure

Chlorine Extraction for ^{36}Cl

From Marek Zreda's lab, University of Arizona

1) Clean teflon bottles using "fantastic" and a soft sponge, rinse in tap water then three times in D.I. water, then rinse using 300 ml hot HNO_3 + 50 ml H_2O_2

2) Weigh 100 g of crushed and seived (0.25 – 1.0 mm) sample into a 1 L teflon bottle

3) Add 20 ml of 0.1 M $AgNO_3$

4) Add 100 ml HNO_3

5) Add a total of 250 ml HF by adding 50 ml at a time and allowing the strongly exothermic process to cool between additions. Cap bottles lightly between additions

6) Close the bottles and put it ona hot plate for 48 hours. Shake periodically. Chlorine will be liberated from the rock matrix and precipitate as AgCl.

7) After complete dissolution, the acid at the top of the bottle can be removed and the heavier precipitate moved to a 250 ml teflon centrifuge tube

8) Centrifuge at 1500 rpm for about 15 minutes

9) Decant the solution and repeatedly rinse the sediment in mill-eq water and centrifuge until the pH is close to neutral

10) Add NH_4OH to dissolve AgCl. Solution must be very basic

11) Centrifuge at 2500 rpm for 10 minutes to separate silicic acid from the solution

12) Transfer the clear solution to a 600 ml teflon beaker. (Keep precipitate in centrifuge bottle in case above 2 steps need to be repeated to improve yield).

13) Carefully add concentrated HNO_3 to reprecipitate AgCl. AgCl will form a milky suspension in acidic solution. Confirm solution is acidic.

14) Place beaker on hot plate for 1 day at 60 C to help AgCl flocculation

15) Carefully remove the solution and rinse the remaining AgCl in mill-eq water

16) Transfer the sample to a 50 ml glass centrifuge tube. Multiple transfers and centrifuges may be necessary. Centrifuge at 1000 rpm for 5 minutes

17) Dissolve the sample in concentrate NH_4OH and add 1 ml $Ba(NO_3)_2$ to precipitate $BaSO_4$. Leave solution for at least 8 hours (preferably longer).

18) Centrifuge the glass tube at 2500 rpm for 10 minutes

19) Carefully remove the solution using clean glass pipette, place it in another glass centrifuge tube and label twice

20) Add sufficent ammount of HNO_3 to precipitate AgCl and let stand for 2 hours

21) Centrifuge, remove acidic solution, and rinse the AgCl at least 3 times in mill-eq. Make sure the final rinse has neutral pH.

22) If samples have high sulfur content, repeat last five steps at least once more.

23) Transfer AgCl onto a clean watch glass. Remove excess water using a pipette. Cover 80% of watchglass with aluminum foil and place sample in 60 C oven for 24 hours.

24) Once dried, the AgCl may be loaded into the AMS targets and weighed

APPENDIX C

Beryllium Extraction from Quartz Seperates

Beryllium Extraction from Quartz Separates

From Devendra Lal and Weiquan Dong Scripps Institute Ca.

1) Separate quartz using Kohl & Nishizumi or Lal's extraction techniques

2) In 200 ml Teflon beaker add approximately 10 g of sample and add 15 ml HF

3) Place beakers on 150 °C hot plate, cover about 85%, heat to near dryness

4) Repeat steps 2 & 3 once more

5) Fume with aprox. 1 ml of $HClO_4$, cover and put on hotplate for 30 minutes

6) Weigh 50 ml centrifuge tubes and record mass

7) Rinse beaker repeatedly with up to 40 ml 6N HCl into the centrifuge tube

8) Balance centrifuge tubes and centrifuge at high rpm for 15 minutes

9) Prepare column by adding 4 volumes (~80 ml) of 6N HCl, then 4 vol. 0.1 N HCl

10) After centrifuging, decant solution to a second tube, measure solution weight. Discard the precipitate

11) Remove $1/10^{th}$ of the solution for ^{9}Be analysis (OPTIONAL)

12) Add aprox. 1.5 mg ^{9}Be (Lal's carrier was .52 mg Be/g so we added 3 g carrier) cap and shake

13) Precipitate slowly with NH_4OH to a pH of 8.2. May have to separate into 2 vials

14) Centrifuge and decant solution. Keep the white gel at bottom

15) Add 1.1 N HCl to one of the split samples and combine again into 1 vial up to aprox. 15 ml

16) Add samples to the clean columns. Once sample has run through funnel, add 3 pore volumes (60 ml) 1.1 N HCl. Beryllium breakthrough is around 60-80 ml

17) When first 3 volumes has run through, add 4 more volumes 1.1 N HCl & change catching beaker to a teflon beaker. Beryllium should be in this fraction

18) Once column has drained, heat sample beaker slowly to dryness

19) Fume with 4 drops of $HClO_4$

20) Dry on low to moderate heat

21) Dissolve sample in a few ml of 1.1 N HCl and transfer to centrifuge tube (up to ~20 ml)

22) Re-precipitate with 5-10 ml of NH_4OH (14%), centrifuge and remove solution

23) Transfer clear gel with a couple drops of dilute (4%) NH_4OH to a small silica crucible

24) Dry $Be(OH)_2$ gel slowly (8-12 hours) under hot light bulb to avoid spattering in furnace

25) Place dried sample into furnace, heat to 950 °C and hold temp 30 minutes (45-60 min total)

26) Remaining sample should be pure BeO. Handle carefully and do not ingest or inhale.

APPENDIX D

Beryllium Extraction from Soil

Beryllium Extraction from Soil

From Devendra Lal and Weiquan Dong Scripps Institute Ca.

1) Measure 2 g of soil (<0.25 mm mesh) sample into a teflon beaker

2) Add ~ 10 ml HF, cover mostly and heat. Add additional HF stepwise as necessary to completely dissolve soil. Heat slowly to dryness.

3) Add 1-2 ml of perchloric to fume, cover, and dry on medium heat

4) Repeat fuming at least once more to remove organics, sample should become lighter in color

5) Re-dissolve sample in 6N HCl and transfer into 50 ml centrifuge tube. Use a teflon scraper and small amounts of acid to insure complete transfer of sample. Catch up to ~ 40 ml.

6) Centrifuge 10 minutes at high speed and decant solution to second set of centrifuge tubes.

7) Add 5-10 ml of 6N HCl and extract a second time, centrifuge and add solution to first tube.

8) Measure solution weight

9) Remove 3-5 g of solution for Be-9 analysis, weigh and record

10) Add ~ 1.5 g of Be-9 carrier (3 g of 0.5 mg/g)

11) Transfer to a 250 ml glass flask and add 40-60 ml EDTA

12) Add 20% NaOH to neutralize solution

13) Add 1.5 ml Acetyl Acetone

14) Cap securely and shake on orbital shaker for ½ hour

15) Add 30 ml Chloroform and shake for 20 minutes

16) Pour sample into 250 ml separator funnel and remove dense portion (at bottom) to teflon a beaker. Dense portion should be transferred back to the glass flask in case procedure needs to be duplicated

17) Pour dense portion back to seperatory funnel and add 30 ml of 8.5 N HCl shake vigorously for 2-3 minutes. Beryllium will go into solution in the strong acid and the chloroform will settle to the bottom.

18) Remove dense portion to glass flask and transfer lighter portion to a teflon beaker.

19) Add sample to column, dry and convert BeOH to BeO as in quartz procedure (steps 17-26)

APPENDIX E

Sample Geochmistry

XRAL Sample Chemistry Results

APPENDIX E

BISHOP CREEK RESULTS														
SAMPLE	B ppm	Na2O %	MgO %	Al2O3 %	SiO2 %	P2O5 %	K2O %	CaO %	TiO2 %	Cr2O3 %	MnO %	Fe2O3 %	LOI %	
BPCR96-1	ND	3.04	0.65	13.1	73.4	0.03	2.96	2.77	0.24	0.01	0.03	2.8	0.95	100.0
2	ND	3.44	0.38	15.0	72.5	0.02	3.47	2.80	0.18	0.02	0.01	1.58	0.65	100.1
3	ND	3.04	0.59	13.1	74.7	0.02	3.18	2.49	0.21	0.01	0.02	1.91	0.6	99.9
4	ND	3.40	0.42	14.2	72.9	0.02	3.45	2.60	0.16	0.02	0.02	1.7	0.6	99.5
5	ND	3.27	0.45	14.2	72.7	0.02	3.30	2.62	0.20	0.01	0.02	1.92	0.75	99.5
6	ND	3.33	0.52	14.5	72.8	0.02	3.49	2.72	0.19	0.03	0.02	1.7	0.8	100.1
7	ND	3.50	0.38	15.2	72.1	0.02	3.52	2.83	0.18	0.03	0.02	1.62	0.4	99.8
8	ND	3.38	0.44	14.8	71.6	0.02	3.52	2.75	0.18	0.07	0.02	1.84	0.65	99.3
9	ND	3.46	0.45	15.2	71.7	0.02	3.68	2.77	0.18	0.02	0.02	1.71	0.25	99.5
10	ND	3.59	0.75	15.2	69.9	0.03	3.17	3.09	0.34	0.03	0.04	2.78	0.75	99.7
11	ND	3.65	0.84	15.2	69.4	0.03	3.25	3.07	0.32	0.03	0.03	2.82	0.7	99.3
12	33.5	3.71	0.34	15.3	70.8	0.02	3.54	2.85	0.18	0.02	0.01	1.59	0.75	99.1
13	ND	3.83	0.58	16.2	68.9	0.02	3.35	3.39	0.24	0.02	0.03	2.15	0.7	99.4
14	ND	3.73	0.88	16.2	68.2	0.03	2.92	3.87	0.29	0.03	0.03	2.62	0.7	99.5
15	28.5	3.36	0.44	14.5	72.8	0.03	3.37	2.93	0.23	0.02	0.02	1.81	0.5	100.0
16	ND	3.26	0.84	13.7	72.2	0.04	3.19	3.56	0.20	0.02	0.03	1.61	1.05	99.7
17	ND	3.57	0.74	14.1	72.9	0.02	3.50	2.66	0.18	0.02	0.02	1.51	0.6	99.8
18	ND	3.42	0.7	13.9	73.0	0.03	3.26	2.84	0.19	0.01	0.02	1.68	0.8	99.9
19	ND	3.20	0.96	13.0	73.6	0.07	3.36	2.59	0.26	0.01	0.02	1.62	1.2	99.9
25	ND	3.59	0.66	15.3	70.1	0.02	3.39	3.13	0.28	0.01	0.02	2.04	0.75	99.3
28	ND	3.52	0.27	15.4	71.4	0.02	4.02	2.71	0.14	0.01	0.01	1.18	0.75	99.4
31	ND	3.38	0.57	15.0	70.5	0.02	3.65	3.62	0.19	0.01	0.02	1.58	0.6	99.1
34	ND	3.25	0.64	14.5	72.4	0.02	3.41	2.99	0.29	0.01	0.02	2.01	0.5	100.0
37	ND	3.43	0.42	15.2	71.0	0.01	3.48	3.19	0.25	0.01	0.02	1.75	0.55	99.3
40	ND	3.61	0.36	15.8	70.8	0.01	3.68	3.24	0.22	0.01	0.02	1.51	0.45	99.7
43	ND	3.49	0.18	15.7	71.9	0.01	4.04	2.78	0.13	0.01	0.01	1.14	0.35	99.7
BPCR96 P-1	ND	3.24	0.61	14.3	72.1	0.03	3.39	2.79	0.24	0.01	0.03	2.04	1.10	99.9
P-2	ND	3.46	0.53	14.6	72.0	0.02	3.33	2.85	0.20	0.01	0.02	1.85	0.85	99.7
P-3	ND	3.43	0.48	14.5	72.3	0.02	3.33	2.87	0.19	0.01	0.02	1.85	1.00	100.0
P-4	ND	3.31	0.67	14.5	71.9	0.02	3.15	3.18	0.26	0.01	0.02	2.28	0.85	100.2
P-5	ND	3.29	0.41	14.0	73.5	0.02	3.52	2.47	0.18	0.01	0.02	1.7	0.65	99.8
P-6	ND	3.28	0.52	13.9	73.3	0.02	3.52	2.59	0.20	0.01	0.02	1.95	0.75	100.1
P-7	ND	3.36	0.54	14.2	72.3	0.03	3.48	2.75	0.23	0.03	0.02	2.46	0.60	100.0
P-8	ND	3.36	0.52	14.1	73.3	0.02	3.16	2.83	0.22	0.02	0.02	2.22	0.40	100.2
P-9	ND	3.54	0.57	14.7	71.5	0.02	3.22	3.06	0.18	0.03	0.02	2.05	0.40	99.3

APPENDIX F

^{36}Cl Results

SAMPLE	LAB I.D.	Depth (cm)	Surface	$^{36}Cl/^{35}Cl$ (10^{-15})	% error
BPCR96-1	S96-1197	0-5	Qthy	1250 ± 70	5.6
BPCR96-2	S96-1198	20-25		1290 ± 80	6.2
BPCR96-3	S96-1199	40-45		1230 ± 80	6.5
BPCR96-4	S96-1200	0-5	Qthy	1620 ± 130	8.0
BPCR96-5	S96-1201	20-25		1310 ± 60	4.6
BPCR96-6	S96-1202	40-45		1270 ± 180	14.2
BPCR96-7	S96-1203	0-5	Qtho	1570 ± 60	3.8
BPCR96-8	S96-1204	20-25		1405 ± 59	4.2
BPCR96-9	S96-1205	40-45		1380 ± 180	13.0
BPCR96-10	R96-1226	0-5	Qbuy	100 ± 1400	1400.0
BPCR96-11	R96-1227	20-25		1400 ± 90	6.4
BPCR96-12	R96-1228	40-45		1630 ± 90	5.5
BPCR96-13	R96-1229	0-5	Qsc	833 ± 56	6.7
BPCR96-14	R96-1230	20-25		613 ± 44	7.2
BPCR96-15	R96-1231	40-45		785 ± 39	5.0
BPCR96-16	R96-1232	0-5	Qc	1636 ± 66.9	4.1
BPCR96-17	R96-1233	20-25		1390 ± 80	5.8
BPCR96-18	Not Measured	40-45			
BPCR96-19	S98-0388	0-5	Qby	833 ±26	3.1
BPCR96-20	Not Measured	20-25			
BPCR96-21	Not Measured	40-45			
BPCR96 22 to 24	No Sample				
BPCR96-25	R96-1234	0-5	Qtho?	855 ± 39	4.6
BPCR96-26	Not Measured	20-25			
BPCR96-27	Not Measured	40-45			
BPCR96-28	R96-1235	0-5	Qbo	2100 ± 120	5.7
BPCR96-29	Not Measured	20-25			
BPCR96-30	Not Measured	40-45			
BPCR96-31	R96-1236	0-5	Qle	832 ± 55	6.6
BPCR96-32	Not Measured	20-25			
BPCR96-33	Not Measured	40-45			
BPCR96-34	R96-1237	0-5	Qbi	1280 ± 60	4.7
BPCR96-35	Not Measured	20-25			
BPCR96-36	Not Measured	40-45			
BPCR95-OBVS3	S98-0387			873 ± 33	3.8
BPCR95-OBVS1	S98-0386			1054 ± 42	4.0

DEEP SOIL PITS

SAMPLE	LAB I.D.	Depth	Surface	$^{36}Cl/^{35}Cl$	% error
Younger Tungsten Hills					
BPCR96 P-1	S96-1192	0-15 cm	Qthy	1277 ± 53	4.2
BPCR96 P-2	S96-1193	15-30	Qthy	1503 ± 55	3.7
BPCR96 P-3	S96-1194	30-45	Qthy	350 ± 70	20.0
BPCR96 P-4	S96-1195	45-60	Qthy	1100 ± 60	5.5
BPCR96 P-5	S96-1196	60-75	Qthy	1008 ± 55	5.5
BPCR96 P-6	Not Measured	75-90	Qthy		
BPCR96 P-7	Not Measured	90-105	Qthy		
BPCR96 P-8	Not Measured	105-120	Qthy		
BPCR96 P-9	Not Measured	120-135	Qthy		
Older Bishop					
BPCR96 P-10	S98-0389	0-5	Qbo	996 ± 44	4.4
BPCR96 P-11	S98-0390	5-10	Qbo	518 ± 25	4.8
BPCR96 P-12	Not Measured	10-15	Qbo		
BPCR96 P-13	S98-0391	15-20	Qbo	585 ± 29	5.0
BPCR96 P-14	S98-0392	20-25	Qbo	577 ± 29	5.0
BPCR96 P-15	S98-0393	30-35	Qbo	540 ± 24	4.4
BPCR96 P-16	S98-0394	35-40	Qbo	469 ± 26	5.5
BPCR96 P-17	S98-0395	40-45	Qbo	426 ± 30	7.0
BPCR96 P-18	S98-0396	50-55	Qbo	349 ± 18	5.2
BPCR96 P-19	S98-0397	55-60	Qbo	323 ± 17	5.3
Older Tungsten Hills					
BPCR96 P-20	S98-0398	0-5	Qtho	760 ± 260	34.2
BPCR96 P-21	S98-0399	5-10	Qtho	1230 ± 60	4.9
BPCR96 P-22	S98-0400	10-15	Qtho	1072 ± 56	5.2
BPCR96 P-23	S98-0401	15-20	Qtho	1252 ± 31	2.5
BPCR96 P-24	S98-0402	20-25	Qtho	1297 ± 32	2.5
BPCR96 P-25	S98-0403	25-30	Qtho	699 ± 55	7.9
BPCR96 P-26	S98-0404	30-35	Qtho	812 ± 22	2.7
BPCR96 P-27	S98-0405	35-40	Qtho	723 ± 21	2.9
BPCR96 P-28	S98-0406	40-45	Qtho	554 ± 25	4.5
BPCR96 P-29	S98-0407	45-50	Qtho	536 ± 23	4.3

APPENDIX G

^{10}Be Results

SAMPLE	LAB I.D.	Depth (cm)	Surface	$^{10}Be/^{9}Be$	% error
BPCR96-1	S98-0970	0-5	Qthy	42 ± 8	19.0
BPCR96-4	S98-0971	0-5	Qthy	58 ± 12	20.7
BPCR96-6	S98-0972	40-45	Qthy	47 ± 13	27.7
BPCR96-7	S98-0974	0-5	Qtho	55 ± 11	20.0
BPCR96-10	S98-0975	0-5	Qbuy	51 ± 15	29.4
BPCR96-13	S98-0976	0-5	Qsc	28 ± 15	53.6
BPCR96-15	S98-0977	40-45	Qsc	20 ± 11	55.0
BPCR96-16	S98-0979	0-5	Qc	49 ± 11	22.4
BPCR96-19	S98-0980	0-5	Qby	10 ± 8	80.0
BPCR96-28	S98-0981	0-5	Qbo	71 ± 10	14.1
BPCR96-31	S98-0982	0-5	Qle	25 ± 9	36.0
BPCR96-34	S98-0984	0-5	Qbi	29 ± 9	31.0
BPCR96-37	S98-0985	0-5	Qthy	30 ± 9	30.0
BPCR96-40	S98-0986	0-5	Qthy	32 ± 9	28.1
DEEP SOIL PITS					
SAMPLE	LAB I.D.	Depth	Surface	$^{10}Be/^{9}Be$	% error
BPCR96 P-1	S96-0987	0-15 cm	Qthy	3340 ± 13	0.4
BPCR96 P-2	S96-0989	15-30	Qthy	3180 ± 90	2.8
BPCR96 P-3	S96-0990	30-45	Qthy	1900 ± 70	3.7
BPCR96 P-4	S96-0991	45-60	Qthy	798 ± 29	3.6
BPCR96 P-5	S96-0992	60-75	Qthy	277 ± 16	5.8
BPCR96 P-6	S98-0994	75-90	Qthy	140 ± 17	12.1
BPCR96 P-7	S98-0995	90-105	Qthy	79 ± 12	15.2
BPCR96 P-8	S98-0996	105-120	Qthy	167 ± 17	10.2
BPCR96 P-9	S98-0997	120-135	Qthy	160 ± 13	8.1
BPCR96 P-10	S98-0998	0-15	Qbo	1350 ± 80	5.9
BPCR96 P-11	S98-0999	15-30	Qbo	668 ± 29	4.3
BPCR96 P-13	S98-1000	45-60	Qbo	224 ± 14	6.3
BPCR96 P-15	S98-1001	75-90	Qbo	131 ± 13	9.9
BPCR96 P-17	S98-1002	105-120	Qbo	47 ± 10	21.3
BPCR96 P-19	S98-1004	145-160	Qbo	54 ± 21	38.9
BPCR96 P-20	S98-1005	0-15	Qtho	1510 ± 12	0.8
BPCR96 P-22	S98-1006	30-45	Qtho	651 ± 42	6.5
BPCR96 P-24	S98-1007	60-75	Qtho	140 ± 18	12.9
BPCR96 P-27	S98-1008	90-105	Qtho	70 ± 16	22.9
BPCR96 P-29	S98-1009	120-135	Qtho	38 ± 10	26.3

REFERENCES

Anderson, M. A., Bertsch, P. M., and Miller, W. P., 1990, Beryllium in selected southeastern soils: Journal of Environmental Quality, v. 19, p. 347-348.

Aruscavage, P. J., and Campbell, E. Y., 1983, An Ion-selective electrode method for determination of chlorine in geological materials: Talanta, v. 30, p. 745-749.

Barg, E., 1992, Studies of Beryllium Geochemistry in Soils: Feasibility of using Be-10/Be-9 Ratios for Age Determination: Unpub. PhD thesis, Scripps Institute of Oceanography 181 p.

Bebeshko, G. I., and Nesterina, E. M., 1993, Ion-selective electrode potentiometric determination of chlorine in rocks: Journal of Analytical Chemistry, v. 49, p. 584-586.

Benson, L., Burdett, J., and Phillips, F., et al, 1996, Climatic and hydrologic oscillations in the Owens Lake Basin and adjacent Sierra Nevada, California: Science, v. 274, p. 746-749.

Bentley, H., Phillips, F., Davis, S., Elmore, D., and et. al, 1986, Chlorine 36 dating of very old groundwater: the Great Artesian Basin, Australia: Water Resources Research, v. 22, p. 1991-2001.

Bentley, H. W., Davis, S. N., Elmore, D., and Phillips, F. M., 1982, Thermonuclear Cl-36 pulse in natural water: Nature, v. 300, p. 737-740.

Brown, L., 1987, Be-10 as a tracer of erosion and sediment transport: Chemical Geology, v. 65, p. 189-196.

Brown, L., Silver, J. N., Pavich, M., Klein, J., and Middleton, R., 1986, Detection of erosion events using Be-10 profiles: example of the impact of agriculture on soil erosion in the Chesapaeke Bay area: Earth and Planetary Science Letters, v. 80, p. 82-90.

Brown, L., Stensland, G. J., Klein, J., and Middleton, R., 1989, Atmospheric deposition of Be-7 and Be-10: Geochimica et Cosmochimica Acta, v. 53, p. 135-142.

Cerling, T. E., and Craig, H., 1994, Geomorphology and in-situ cosmogenic isotopes: Ann. Rev. Earth Planetary Sci., v. 22, p. 273-317.

Dansgaard, W., and al, e., 1993, Evidence for general instability of past climate from a 250-kyr ice-core record: Nature, v. 364, p. 218-220.

Davis, R., and Schaefer, O. A., 1955, Chlorine-36 in nature: Annual New York Academy of Science, p. 105-122.

Davis, S. N., and Murphy, E., 1987, Dating ground water and the evaluation of repositories for radioactive waste, Tucson, Office of Nuclear Regulatory Research.

Elmore, D., and Phillips, F. M., 1987, Accelerator mass spectrometry for measurement of long-lived radioisotopes: Science, v. 23, p. 543-550.

Elmore, D., and Sharma, P., 1997, Status and Plans for the PRIME lab and AMS facility: Nuclear Instruments and Methods in Physics Research B, v. 123, p. 69-72.

Fabryka-Martin, J. T., 1988, Production of Radionuclides in the Earth and their Hydrogeologic Significance with emphasis on Cl-36 and I-129: Unpub. Ph.D. dissertation thesis, University of Arizona.

Gu, Z. Y., Lal, D., and al, e., 1996, Five million year Be-10 record in Chinese loess and red-clay: Climate and weathering relationships: Earth and Planetary Science Letters, v. 144, p. 273-287.

Gunnell, Y., 1998, Present, past and potential denudation rates; is there a link? Tentative evidence from fission track data, river sediment loads and terrain analysis in the South Island Shield.: Geomorphology, v. 25, p. 135-153.

Kohl, C. P., and Nishiizumi, K., 1992, Chemical Isolation of Quartz for Measurement of in-situ produced Cosmogenic Nuclides: Geochimica et Cosmochimica Acta, v. 56, p. 3583-3587.

Kurz, M. D., and Brook, E. J., 1994, Surface Exposure Dating with Cosmogenic Nuclides, *in* Beck, C., ed., Dating in Exposed and Surface Contexts, Albuquerque, University of New Mexico Press, p. 139-159.

Lal, D., 1988, In-situ produced cosmogenic isotopes in terrestrial rocks: Ann. Rev. Earth Planet Sci., v. 16, p. 355-388.

Lal, D., 1991, Cosmic Ray Labeling of Erosion Surfaces: in situ Nuclide Production Rates and Erosion Models: Earth and Planetary Science Letters, v. 104, p. 424-439.

Lal, D., Pavich, M., Gu, Z. Y., Jull, J. T., and al., e., 1996, Recent Erosional History of a Soil Profile based on Cosmogenic in-situ Radionuclides C-14 and Be-10, Earth Processes: Reading the Isotopic Code, American Geophysical Union, p. 371-376.

Lal, D., and Peters, B., 1967, Cosmic Ray Produced Radioactivity on the Earth, *Encyclopedia of Physics*,edited by S. Fluegge, vol. 46/1, Cosmic Rays II, pp 551-612, Springer Verlag, New York

Lal, D., Peters, B., and Malhotra, P. K., 1957, On the Production of radioisotopes in the atmosphere by cosmic radiation and their application to metereology: Journal of Atmospheric and Terrestrial Physics, v. 12, p. 306-328.

Liu, B., Phillips, F., Fabryka-Martin, J., and Fowler, M., 1994, Cosmogenic Cl-36 Accumulation in Unstable Landforms: Effects of the Thermal Neutron Distribution: Water Resources Research, v. 30, p. 3115-3125.

Louvat, P., and Allegre, C.-J., 1997, Present denudation rates on the island of Reunion determined by river geochemistry, basalt weathering, and mass budget between chemical and mechanical erosions: Geochimica et Cosmochemica Acta, v. 61, p. 3645-3669.

McHargue, L., and Damon, P. E., 1991, The Global Beryllium-10 Cycle: Reviews of Geophysics, v. 29, p. 141-158.

Miller, D., and P., B., 1992, Soil Catena Variation along Alpine Climatic Transect Northern Peruvian Andes: Geoderma, v. 55, p. 211-223.

Monaghan, M., 1987, Greenland ice Be-10 concentrations and average precipitation rates north of 40 degrees north to 45 degrees north: Earth and Planetary Science Letters, v. 84, p. 197-203.

Monaghan, M., Krishnaswami, S., and Turekian, K., 1986, The global average production rate of Be-10: Earth and Planetary Science Letters, v. 76, p. 279-287.

Monaghan, M. C., and Elmore, D., 1994, "Garden Variety" Be-10 in soils on hill slopes: Nuclear Instruments and Methods in Physics Research, v. B92, p. 357-361.

Monaghan, M. C., Krishnaswami, S., and Thomas, J. H., 1983, Be-10 Concentrations and the long-term fate of particle-reactive nuclides in five soil profiles in California: Earth and Planetary Science Letters, v. 65, p. 51-60.

Nishiizumi, K., Klein, J., Kohl, C. P., and Finkel, R. C., 1996, Cosmogenic production of Be-7 and Be-10 in water targets: Journal of Geophysical Research, v. 101, p. 22225-22232.

Nishiizumi, K., Klein, J., Kohl, C. P., Middleton, R., Arnold, J. R., and Fink, D., 1991a, Cosmic Ray Produced Be-10 and Al-26 in Antarctic Rocks: Exposure and Erosion History: Earth and Planetary Science Letters, v. 104, p. 440-454.

Nishiizumi, K., Kohl, C. P., Arnold, J. R., Klein, J., Fink, D., and Middleton, R., 1991b, Cosmic Ray Produced Be-10 and Al-26 in Antarctic Rocks: exposure and Erosion History: Earth and Planetary Science Letters, p. 440-454.

Nishiizumi, K., Lal, D., Klein, J., Middleton, R., and Arnold, J. R., 1986, Production of Be-10 and Al-26 by Cosmic Rays in Terrestrial Quartz in situ and Implications for Erosion Rates: Nature, v. 319, p. 134-136.

Nishiizumi, K., Winterer, E. L., Kohl, C. P., and Klein, J., 1989, Cosmic Ray Production Rates of Be-10 and Al-26 in Quartz from Glacially Polished rocks: Journal of Geophysical research, v. 94, p. 17,907-17,915.

Pavich, M., Brown, L., Harden, J., Klein, J., and Middleton, R., 1986, Be-10 distribution in soils from Merced River Terraces, California: Geochimica et Cosmochimica Acta, v. 50, p. 1727-1735.

Pavich, M. J., Brown, L., Klein, J., and Middleton, R., 1984, Be-10 Accumulation in a Soil Chronosequence: Earth and Planetary Science Letters, v. 68, p. 198-204.

Pavich, M. J., Brown, L., Silver, J. N., Klein, J., and Muddleton, R., 1985, Be-10 Analysis of a Quaternary Wethering Profile in the Virginia Piedmont: Geology, v. 13.

Phillips, F. M., and Elmore, D., et al, 1986, The accumulation of cosmogenic Chlorine-36 in rocks: a method for surface exposure dating: Science, v. 231, p. 41-43.

Phillips, F. M., and Plummer, M., 1996, CHLOE: A program for interpreting in-situ cosmogenic nuclide data for surface exposure dating and erosion studies (abstract): Radiocarbon, v. 38, p. 98.

Phillips, F. M., Plummer, M. A., and Zreda, M., 1998, Preliminary report on Cl-36 Geochronology of Glacial Deposits in the Bishop Creek Drainage, Eastern Sierra Nevada: personal communication

Phillips, F. M., Zreda, M., Flinsch, M., Sharma, P., and Elmore, D., 1996, A reevaluation of cosmogenic Cl-36 production rates in terrestrial rocks: Geophysical Research Letters, v. 23, p. 949-952.

Phillips, F. M., Zreda, M., Smith, S., Elmore, D., Sharma, P., and Kubik, P., 1990, Cosmogenic Cl-36 chronology for glacial deposits at Bloody Canyon, Eastern Sierra Nevada: Science, v. 248, p. 1529-1532.

Raisbeck, G. M., and Yiou, F., 1984, Production of long-lived cosmogenic nuclei and their applications: Nuclear Instruments and Methods in Physics Research, p. 91-99.

Raisbeck, G. M., Yiou, F., Bard, E., Jouzel, J., and Petit, J. R., 1992, Be-10 Deposition at Vostok Antarctica during the last 50,000 years and its relationship to possible cosmogenic production variations during this period, *in* Bard, E., and Broecker, W., eds., The Last Deglaciation: Absolute and Radiocarbon Chronology, Heidelberg, Springer, p. 127-139.

Reyss, J. L., Yokoyama, Y., and Guichard, F., 1981, Production Cross Sections of Al-26, Na-22, Be-7 from Argon and of Be-10, Be-7 from Nitrogen: Implications for the Productions Rates of Al-26 and Be-10 in the Atmosphere: Earth and Planetary Science Letters, v. 53, p. 203-210.

Ritter, D., 1967, Rates of denudation: Jour. of Geol. Educ., v. 15, p. 154-159.

Ritter, D. F., 1978, Process Geomorphology: Dubuque, Wm. C. Brown Publishers, 579 p.

Roessner-Sigrid, and Strecker-Manfred, 1997, Late Cenozoic tectonics and denudation in the central Kenya Rift; quantification of long-term denudation rates: Tectonophysics, v. 278, p. 83-94.

Summerfield, M. A., and Hulton, N. J., 1994, Natural controls of fluvial denudation rates in major world drainage basins: Journal of Geophys. Res., v. 99, p. 13,871-13,883.

Yokoyama, Y., Reyss, J.-L., and Francois, G., 1977, Production of Radionuclides by Cosmic Rays at Mountain Altitudes: Earth and Planetary Science Letters, v. 36, p. 48-50.

Zreda, M., England, J., Elmore, D., Phillips, F. M., and Sharma, P., 1999, Unblocking of the Nares Strait by Greenland and Ellesmere ice-sheet retreat 10,000 years ago: Nature.

Zreda, M., and Phillips, F., 1994a, Cosmogenic Cl-36 Accumulation in Unstable Landforms: Simulations and Measurements on Eroding Moraines: Water Resource Research, v. 30, p. 3127-3136.

Zreda, M., Phillips, F. M., Elmore, D., Sharma, P., Kubik, P., and Dorn, R., 1991, Cosmogenic Cl-36 production rates in terrestrial rocks: Earth and Planetary Science Letters, v. 105, p. 94-109.

Zreda, M. G., and Phillips, F. M., 1994b, Surface Exposure Dating by Cosmogenic Chlorine-36 Accumulation, *in* Beck, C., ed., Dating in Exposed and Surface Contexts, Albuquerque, University of New Mexico Press, p. 161-183.